Spectrochimica Acta Part A: Molecular and Biomolecular Spectroscopy 181 (2017) 286–308

Contents lists available at ScienceDirect

Spectrochimica Acta Part A: Molecular and Biomolecular Spectroscopy

journal homepage: www.elsevier.com/locate/saa

Infrared spectroscopy of matrix-isolated neutral polycyclic aromatic nitrogen heterocycles: The acridine series

A.L. Mattioda[d,*], C.W. Bauschlicher Jr.[d], A. Ricca[a,d], J. Bregman[a,d], D.M. Hudgins[b], L.J. Allamandola[c,d]

[a] Carl Sagan Center, SETI Institute, 189 Bernardo Ave., Suite 200, Mountain View, CA 94035, United States
[b] NASA HQ, Washington DC 20546, United States
[c] Bay Area Environmental Research Institute, Mail Stop 245-6, United States
[d] NASA Ames Research Center, Moffett Field, CA 94035, United States

ARTICLE INFO

Article history:
Received 3 October 2016
Received in revised form 23 February 2017
Accepted 17 March 2017
Available online 22 March 2017

Keywords:
Infrared
DFT
Matrix isolation

ABSTRACT

The matrix-isolated, mid-infrared spectra of seven acridine-based polycyclic aromatic nitrogen heterocycles (PANHs) have been measured and compared to their non-nitrogen containing parent molecule. The acridine species investigated include acridine, benz[a]acridine, benz[c]acridine, dibenz[a,j]acridine, dibenz[c,h]acridine, dibenz[a,h]acridine and dibenz[a,c]acridine. The previously reported results for 1 and 2-azabenz[a]anthracenes are included for comparison. The experimentally determined band frequencies and intensities are compared with their B3LYP/6–31G(d) values. The overall agreement between experimental and theoretical values is good and in line with our previous investigations. Shifts, typically to the blue, are noted for the C–H out-of-plane (CH_{oop}) motions upon insertion of a nitrogen atom. The formation of a bay region upon addition of additional benzene rings to the anthracene/acridine structure splits the solo hydrogen motions into a bay region solo and an external solo hydrogen, with the bay region solo hydrogen coupling to the quartet hydrogen motions and the external solo hydrogen coupling with the duo hydrogen motions resulting in an extreme decrease in intensity for the CH_{oop} solo hydrogen band when the external hydrogen is replaced by a nitrogen atom. The C–C and C–H in-plane region of this acridine series exhibits the characteristic two fold increase in intensity, noted previously for PANHs. The strong $\approx$1400 cm^{-1} band, which was identified in the previous PANH study, is noted in several molecular species as well as another strong PANH feature between 1480 and 1515 cm^{-1} for several molecules. The presence of these strong bands appear to be primarily responsible for the two-fold increase in the C-H in-plane region's (1100–1600 cm^{-1}) intensity. The C–H stretching region can be characterized by contributions from the solo (bay or external), duo and quartet hydrogens, similar to what was observed in the dibenzopolyacene compounds.

Published by Elsevier B.V.

1. Introduction

Polycyclic Aromatic Hydrocarbons (PAHs) are of interest in terrestrial as well as extraterrestrial environments. In terrestrial environments, PAHs are the by-product of natural (forest and prairie fires, volcanoes) and anthropogenic (fossil fuel combustion, coking plants, asphalt production, etc.) combustion processes. Given their carcinogenic potential, the Environmental Protection Agency (EPA) has listed 16 specific PAHs as priority pollutants [1]. PAHs in extraterrestrial environments form in the outflow of carbon stars and the emission from large PAH molecules, carbon clusters, and carbon nanograins dominates the infrared spectrum from the majority of galatic and extragalatic objects, including regions of massive star formation, the general interstellar medium (ISM), and star-forming spiral galaxies [2,3]. By modulating radiation fields and influencing charge balance in the diffuse ISM and circumstellar disks, PAHs often take part in local extraterrestrial processes [4,5]. In dense molecular clouds PAHs dominate cooling and promote H_2-formation. Inside the Solar System, specific small PAHs (less than 30 carbon atoms) have been identified in particles from Comet Wild 2 [6], meteorites [7,8], asteroids [9,10], interplanetary dust particles (IDPs), and tentatively

* Corresponding author.
E-mail addresses: Andrew.L.Mattioda@nasa.gov (A. Mattioda), Charles.W.Bauschlicher@nasa.gov (C.W. Bauschlicher).

http://dx.doi.org/10.1016/j.saa.2017.03.044
1386-1425/Published by Elsevier B.V.

identified in planetary satellites such as Iapetus and Phoebe [11]. PAHs have also been identified in meteorites both as smaller individual molecules, and as part of the insoluble organic material (IOM), similar to kerogen material found in terrestrial coals [12,13].

The substitution of a nitrogen atom for a carbon or CH group in a PAH creates a PANH (polycyclic aromatic nitrogen heterocycles) and it has been suggested that these species are present in the interstellar medium (ISM) and in planetary bodies [14–16]. In addition, they have been identified in the carbonaceous component of meteorites [17,18]. PANH have been predicted to be a component of tholins on the surface and in the atmosphere of Titan [19–23]. Tholins are also believed to give the reddish hue to the objects of the outer solar system [24,25]. Clearly, there is ample evidence that any comprehensive study of PAHs must also include PANHs.

Given the importance of PAHs, we have undertaken a multi-decade effort to understand the vibrational spectroscopy of these ubiquitous molecules. As part of this continuing mission, we have determined the infrared (IR) spectra of fourteen neutral PAH and PANH (polycyclic aromatic nitrogen heterocycles) molecules using a joint density functional theory-matrix-isolation experimental approach. Shown in Fig. 1, starting with anthracene, we investigate the changes in their vibrational spectral properties as the series grows by the addition of one and two additional benzene rings, creating a benz[a]anthracene and a dibenz[a,j], dibenz[a,h], and dibenz[a,c]anthracene series. We also investigate the spectral changes induced by the presence and position of the endoskeletal nitrogen atom, particularly as it relates to its incorporation into the bay region of the PANH versus an external location.

The remainder of the paper is divided into the following sections: Methods 2 (Experimental and Theoretical), Results and Discussion 3, followed by a Conclusion 4.

2. Methods

The molecules studied are shown Fig. 1 along with several molecules that were studied in previous work, but are expanded upon in this work to illustrate the trends. The molecules contain an anthracene core with one or two benzene rings added to it, forming the benz[a]anthracene, dibenz[a,j]anthracene, dibenz[c,h]anthracene and dibenz[a,c]anthracene. For each molecular series, one CH group is replaced in the parent molecules to form the nitrogen series.

2.1. Experimental Techniques

The matrix-isolation infrared (IR) techniques employed in these studies have been described in detail elsewhere [26–28] and will be briefly summarized here. All samples were isolated in an argon matrix that was prepared by vapor co-deposition of the species of interest with an over abundance of argon (Ar) onto a 15 K CsI window suspended in a high-vacuum chamber ($p < 10^{-7}$ Torr). The PAH and PANH samples were vaporized from heated Pyrex tubes while the argon was admitted through an adjacent length of N_2(l)- trapped copper tubing. The conditions were optimized to produce an Ar/PAH or PANH ratio in excess of 1000:1. An IR spectrum of the sample was recorded once a sufficient amount of neutral material was accumulated, as indicated by the strength of the weakest bands.

Experimental samples were obtained from either Chiron or Resolution Systems, the U.S. supplier for Chiron. All of the PAH and PANH samples were of 99% or greater purity. Spectra were recorded on a Bio-Rad/Digilab Excalibur FTS-4000 IR spectrometer, with each spectrum recorded as a co-addition of 500 scans at a resolution of 0.5 cm^{-1}. For presentation purposes, the reported spectra have been baseline-corrected with several bands resulting from impurities (such as water and purge air) either subtracted or truncated using the Win-IR Pro 3.4 Software package and normalized to 1×10^{16} molecules. All numerical values cited in this paper are based on the band integrations of unaltered data.

The integrated intensities ($\int \tau d\nu$) for the neutral bands were determined using the Win-IR Pro 3.4 (DigiLab) software package. The absolute intensities ($A = (1/N)\int \tau d\nu$), where N is the column density of absorbers (in molecules cm^2), for the experimentally measured PAHs and PANHs were determined using the theoretical values as follows. Integrated intensities for all bands between 1550 and 500 cm^{-1} were summed, obtaining the total absorption intensity for this region. This range was chosen to exclude the contributions of the far-IR bands ($\nu < 500$ cm^{-1}) and the upper cutoff of $\nu > 1550$ cm^{-1} excludes the CH stretching bands, which are substantially overestimated by quantum calculations [3,30], any potential bands from matrix-isolated water contamination, if present, and the overtone/combination bands that are present in the experimental data and not included in the theory, which is restricted to the harmonic approximation. These areas are then put on an absolute footing using theoretically calculated absolute band intensities as described by Hudgins and Sandford [28]. That is, the experimental relative intensities are scaled by the ratio of the sum of the theoretically computed intensities between 1550 and 500 cm^{-1} over the sum of the experimental intensities over the same range.

$$A_i^{\exp} = I_{rel,i}^{\exp}\frac{\sum_{\nu=500}^{1550} A^{thy}}{\sum_{\nu=500}^{1550} I_{rel}^{\exp}}. \quad (1)$$

An advantage of this method is the fact that although there may be some band-to-band variability in the accuracy of the calculated intensity, the total intensity is generally accurate to within 10–20%, excluding theC–H stretching region. The IR spectra for anthracene [26,28,29], acridine [29,30], benz[a]anthracene [28] (or 1,2 benzanthracene) as well as 1 and 2-azabenz[a]anthracene [27] have been previously published but are updated and included here for comparison purposes.

2.2. Theoretical Techniques

The structures have been fully optimized and the harmonic frequencies computed using density functional theory (DFT). We have used the hybrid [31] B3LYP [32] functional. Experience has shown that the hybrid B3LYP functional in conjunction with the 4–31G basis set [33] predicts reliable vibrational frequencies for closed-shell neutral species [34,35], including those that contain nitrogen atoms [26,27]. Despite this success, some preliminary calculations for the ions of the molecules studied in this work suggested that the larger 6–31G(d) basis set was superior for the ions. Therefore the 6–31G(d) was also tested for the neutrals and the results using the larger 6–31G(d) basis set were found to be in better agreement with experiment. Note that all six components of the 3d functions are used. Given the improvement when the size of the basis set was increased, the even larger cc-pVTZ set of Dunning [36] was tested. Excluding one band, discussed below, the 6–31G(d) and cc-pVTZ basis sets gave very similar results and therefore the smaller 6–31G(d) basis set was used.

We previously developed [35] two scaling factors for a variety of basis sets, but the results were disappointing for the larger basis set. Subsequently it was realized that using the same fitting approach, but using three scale factors significantly improved the results. Therefore in this work, three scale factors are used for the B3LYP/6–31G(d) approach. The range 0 to 1111.$\bar{1}$ cm^{-1} is scaled by 0.9821, 1111.$\bar{1}$ to 2500.0 cm^{-1} is scaled by 0.9715, and finally those frequencies greater than 2500.0 cm^{-1} are scaled by 0.9590.

For naphthalene this yields an average and maximum error of 7.2 and 13.0 cm^{-1}, respectively. While these errors are slightly larger than the smaller basis set for naphthalene (4.5 and 12 cm^{-1}, respectively), the 6–31G(d) basis set agrees better with experiment for these nitrogen containing species; this is probably a result of the nitrogen atom in the current work. To compare the computed spectra with experiment, we broaden the computed spectra using a Gaussian function with a full width at half maximum (FWHM) of 5 cm^{-1}.

For naphthalene there are both gas phase [37] and matrix isolation [38,39] experimental spectra. The largest difference between the gas phase [37] and matrix isolation experiment performed at Ames [38] is 14 cm^{-1} for the C–H stretching modes and 5 cm^{-1} for the non-C–H stretching modes. The differences are larger for the other experiment [39], 29 and 12 cm^{-1}, respectively. Therefore some of the differences between theory and experiment many arise from matrix effects, but this should be sufficiently small that we can use theory to identify and characterize the experimental bands.

All calculations have been performed using Gaussian 09 or earlier versions of the same program system [40]. The interactive molecular graphics program Jmol [41] has been used to aid the analysis of the vibrational modes.

3. Results and Discussion

The acridine molecules and their parent PAH molecules that are studied in this investigation are shown in Fig. 1. The study starts with the simple anthracene ($C_{14}H_{10}$) structure with three rings, then adds a fourth ring to form the benz[a]anthracene ($C_{22}H_{14}$) series and a fifth ring, forming the dibenz[a,j], dibenz[a,h], and dibenz[a,c]anthracene ($C_{22}H_{14}$) series. The acridine molecules in each of these series have the nitrogen atom either in an internal bay region (benz[c]acridine ($C_{13}H_9N$), dibenz[c,h]acridine ($C_{21}H_{13}N$), dibenz[a,h]acridine ($C_{21}H_{13}N$), or dibenz[a,c]acridine($C_{21}H_{13}N$)) or external position (benz[a]acridine ($C_{13}H_9N$) or dibenz[a,j]acridine ($C_{21}H_{13}N$)). The positions in the parent PAHs, anthracene, benz[a]anthracene and dibenz [a,j], [a,h] and [a,c] anthracene molecules, are numbered to help aid in the discussion, see molecules 1, 3, 8, 11, and 13 in Fig. 1.

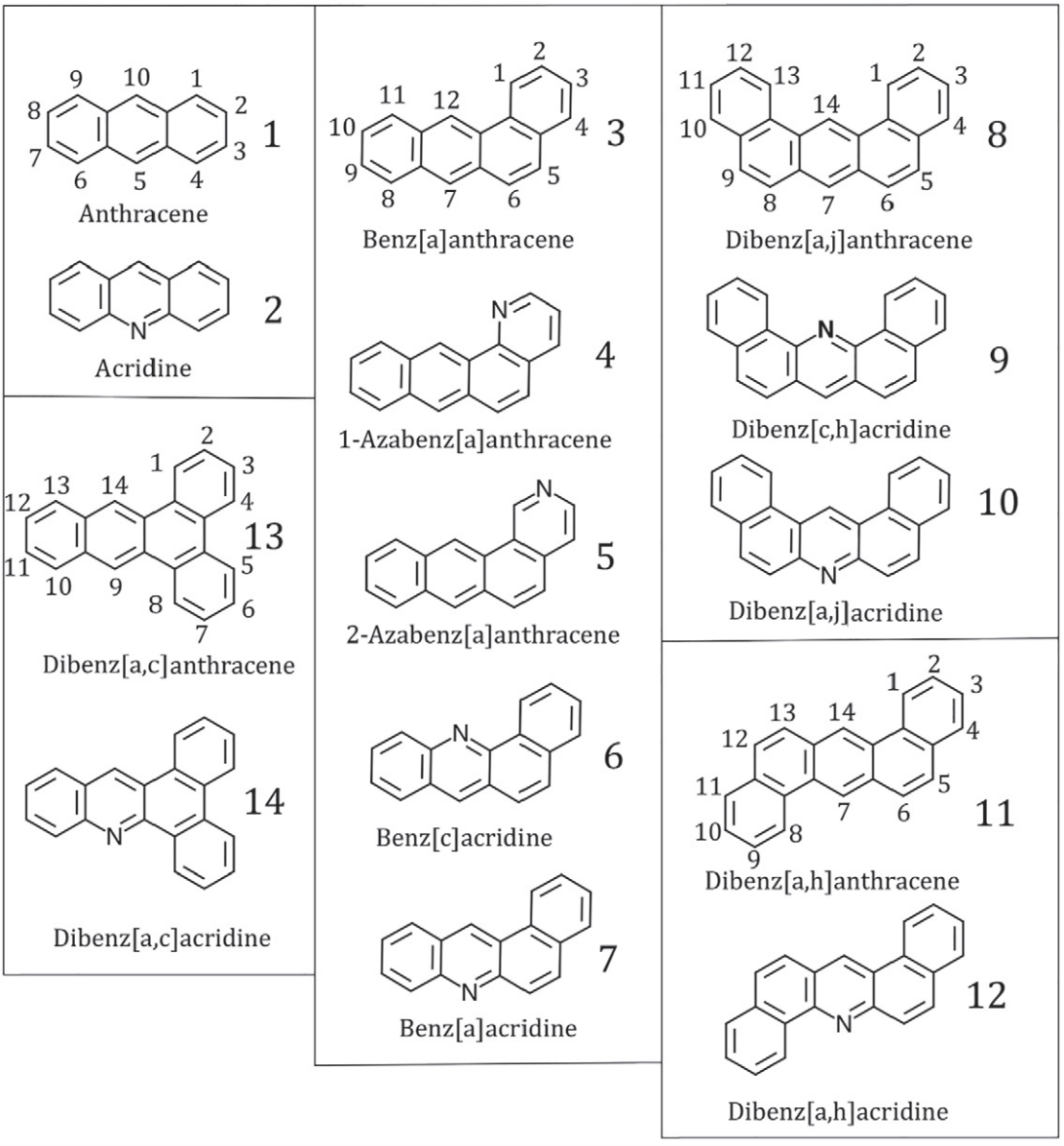

Fig. 1. The molecules included in this investigation and the numbering scheme for the discussion of the vibrational spectra. The series consist of the anthracene, benz[a]anthracene and [a,j], [a,h], and [a,c] dibenzanthracene series.

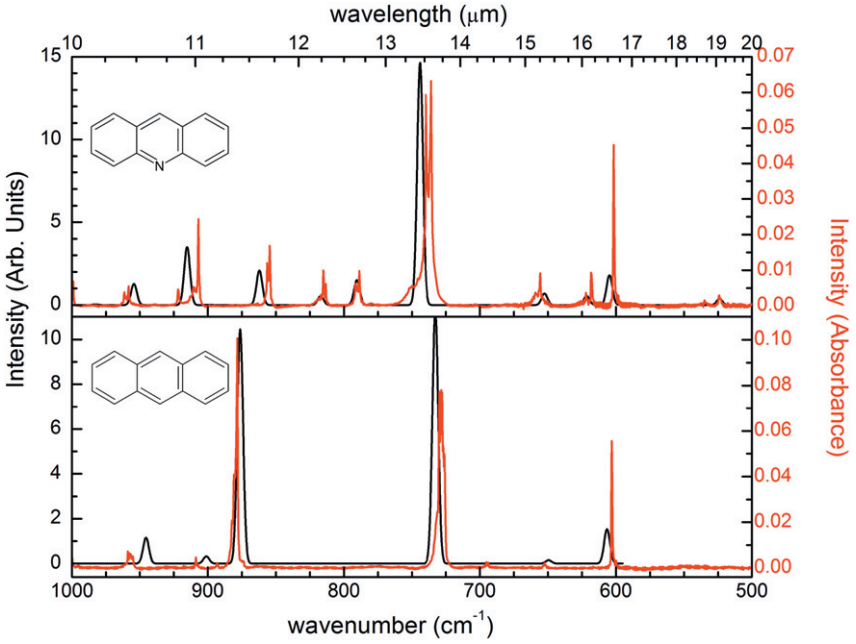

Fig. 2. The 500–1000 cm^{-1} region of the experimental (shown in red) and theoretical (B3LYP/6-31G(d) and shown in black) spectra for anthracene and acridine. Experimental spectra have been normalized to 1×10^{16} molecules.

The numbers will serve as reference points when discussing the spectroscopy of the molecular series.

3.1. The C–H Out-of-Plane(CH_{oop}) and Skeletal Region(450 to 1000 cm^{-1})

In this subsection, we discuss the 450 to 1000 cm^{-1} region of the spectra. However, we were unable to obtain experimental spectra in the 450 to 500 cm^{-1} region for all species. Therefore, only the 500 to 1000 cm^{-1} portion of the experimental and theoretical spectra are shown in Figs. 2–5, but the bands between 450 and 500 cm^{-1} are included in Tables 1–5. In this section, we focus on the experimental data for position and intensity and use the corresponding theory to identify the type of mode.

3.1.1. Addition of Benzene Rings

The theoretical and experimental infrared spectra for anthracene, benz[a]anthracene, and dibenz[a,j], dibenz[a,h], and dibenz[a,c]

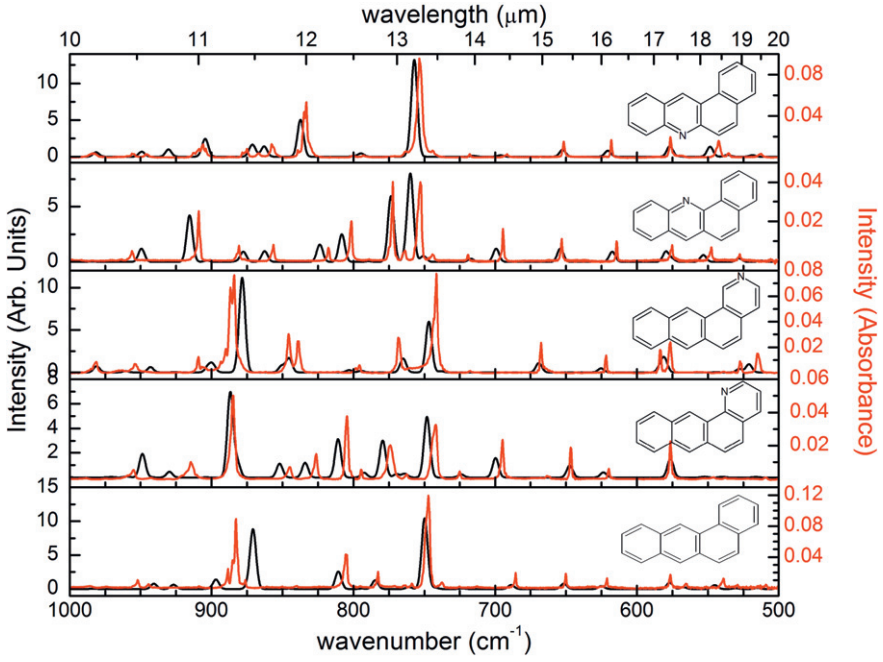

Fig. 3. The 500–1000 cm^{-1} region of the experimental (shown in red) and theoretical (B3LYP/6-31G(d) and shown in black) spectra for the species derived from benz[a]anthracene. Experimental spectra have been normalized to 1×10^{16} molecules.

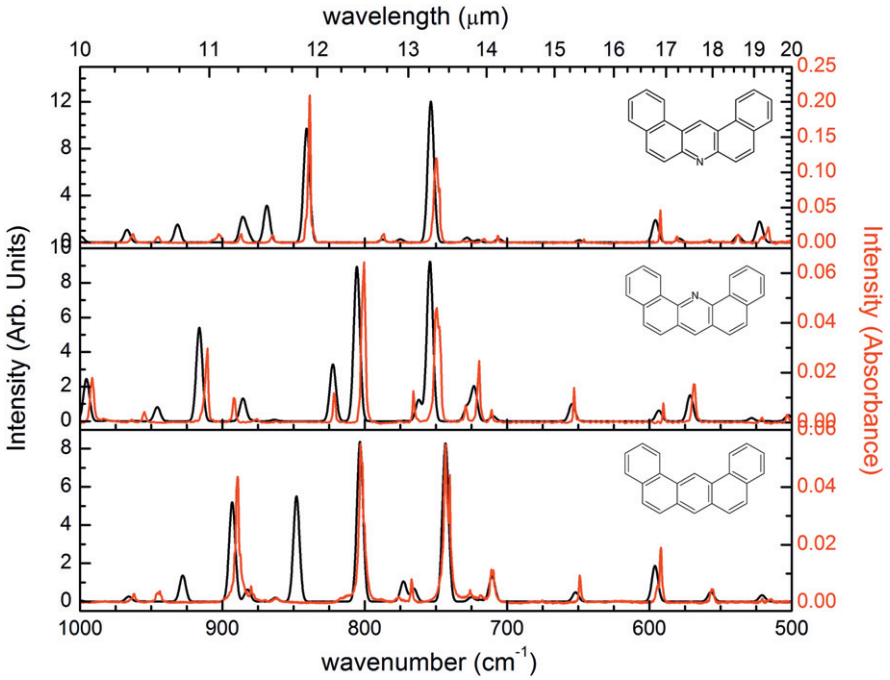

Fig. 4. The 500–1000 cm^{-1} region of the experimental (shown in red) and theoretical (B3LYP/6-31G(d) and shown in black) spectra for the species derived from dibenz[a,j]anthracene. Experimental spectra have been normalized to 1×10^{16} molecules.

anthracene are shown in Figs. 2–5 for the CH out-of-plane region. The bands are tabulated in Tables 1–5. The band positions of anthracene and benz[a]anthracene correspond well with those previously published [28]. The main feature in the anthracene spectrum consists of molecular skeletal modes around 470 and 603 cm^{-1}. The 470 cm^{-1} feature resembles a butterfly motion where the hydrogens and carbon atoms along the long edge of the molecule (4, 5, 6 and 1, 10, 9 in Fig. 1 anthracene) are wagging out of the plane opposite the non-hydrogen bearing carbon atoms. The 603 cm^{-1} band is an anti-symmetric breathing motion of the two end aromatic rings

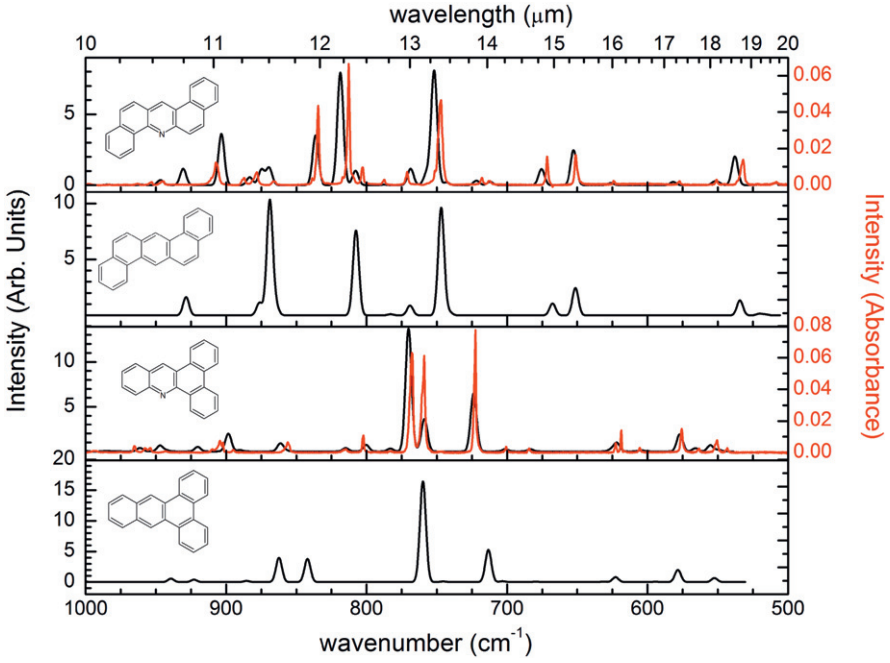

Fig. 5. The 500–1000 cm^{-1} region of the experimental (shown in red) and theoretical (B3LYP/6–31G(d) and shown in black) spectra for the species derived from dibenz[a,h]anthracene and dibenz[a,c]anthracene. Experimental spectra have been normalized to 1×10^{16} molecules.

Table 1
Summary of anthracene and acridine results. The intensities, A, are in km/mol and the band positions are in cm^{-1}. The theoretical results are taken from the B3LYP/6–31G(d) approach.

Anthracene					Acridine				
Experimental		Theory			Experimental		Theory		
Center[a]	A	Center	A	Sym	Center	A	Center	A	Sym
469.6vb	16.3	476.1	12.8	b_{3u}	469.7	2.6	476.8	3.1	b_1
603.0	8.4	606.5	8.2	b_{2u}	601.6	12.8	604.7	9.5	b_2
					618.1	2.8	621.5	2.9	a_1
					655.6	3.2	652.4	3.7	a_1
727.6vb	68.1	732.7	59.7	b_{3u}	735.9	36.8	742.2	0.4	a_1
					739.6	40.3	744.1	77.6	b_1
					788.6*	6.1	790.4	8.0	b_1
					790.2				
					791.4				
					815.1	2.4	817.0	2.9	b_2
878.3	40.9	876.2	55.6	b_{3u}	854.4*	9.1	862.1	11.1	b_1
					866.3				
					906.8	10.0	915.1	17.6	b_1
957.2	6.4	945.3	6.1	b_{3u}	958.2	1.2	954.2	6.8	b_1
					998.9	4.3			
1001.1	7.3	1017.4	3.9	b_{2u}	1000.3*		1014.0	4.2	b_2
					1123.6	1.8	1137.3	2.5	b_2
					1141.5*	7.9	1139.6	9.6	a_1
					1142.8				
1149.5	4.6	1147.5	4.7	b_{1u}	1148.0*	3.4			
					1151.5				
1166.7	4.4	1166.0	1.6	b_{2u}	1169.7	2.2	1172.4	1.5	b_2
1272.7	3.4	1260.9	8.3	b_{1u}			1258.5	1.1	a_1
1318.3	7.6	1309.3	4.2	b_{1u}	1296.4	0.5	1310.4	4.4	b_2
1346.4	1.7	1353.4	4.0	b_{2u}	1374.4*	3.6	1365.3	2.9	b_2
					1379.2				
1449.8	3.2	1457.7	1.2	b_{1u}	1404.8	6.2	1397.7	6.1	a_1
					1442.5*	2.7	1447.0	1.7	b_2
					1443.6				
					1447.0				
1460.3	1.4	1457.9	1.9	b_{2u}	1465.7*	7.6	1468.8	3.8	a_1
					1466.7				
1542.2	6.7	1551.2	4.4	b_{2u}	1518.9	48.2	1529.1	35.9	b_2
					1561.0*	10.0	1558.9	8.7	a_1
					1565.0				
					1582.7	2.6	1588.2	8.1	b_2
1628.2	4.2	1639.1	6.9	b_{1u}	1625.4	17.2	1625.4	15.9	b_2
					1631.5	3.0	1642.5	5.7	a_1
3021	96.8				3018.6	3.4	3041.7	5.7	a_1
3035		3040.7	10.7	b_{1u}	3033.9	68.5	3048.1	9.2	a_1
3049		3046.4	16.5	b_{1u}	3041.1		3058.9	1.3	b_2
3059					3061.5*		3059.1	27.7	a_1
3068*		3063.4	73.5	b_{1u}	3083.4		3073.4	46.6	b_2
		3075.3	77.5	b_{2u}	3095.6		3073.6	15.0	a_1
							3086.7	23.5	b_2
							3087.2	9.6	a_1

[a] vb indicates a very broad band, while a * indicates the band is part of a complex.

(C–H groups 1, 2, 3, 4 and 6, 7, 8, 9 in Fig. 1 anthracene). The bands at 727.6 and 878.3 cm^{-1} are normally attributed to the CH out-of-plane (CH_{oop}) modes for the quartet (aromatic ring with four adjacent hydrogen atoms, i.e. the hydrogens at positions 1–4 and 6–9 in Fig. 1 anthracene) and solo hydrogen (aromatic ring with a single hydrogen atom, see positions 5 and 10) modes of anthracene, respectively. However, for anthracene, the quartet mode also involves the solo hydrogens moving out-of-phase with the quartet's CH_{oop}. For the 878.3 cm^{-1} mode, the solo hydrogens are coupled, in-phase, to the sets of the hydrogen atoms on the ends of the anthracene molecule (positions 2 and 3 and 7 and 8). The weak 908.7 cm^{-1} mode is caused by C–C–C and C–H in-plane rocking motions of the anthracene skeleton, while the 957.2 cm^{-1} mode is a CH_{oop} motion where the hydrogens along the long axis of the molecule (4, 5, 6 and 1, 10, 9) are out-of-phase with the CH_{oop} motion of the hydrogens on the ends (2, 3 and 7, 8).

Several interesting things occur when a benzene ring is attached to the 1, 2 position of anthracene to form benz[a]anthracene (See Fig. 3). First, the skeletal region (≈450 to 700 cm^{-1}) becomes more active with new weak to moderate features appearing around 539.1, 565.3, 576.5, 621.2, 650.2, and 685.5 cm^{-1}. The 539.1, 565.5, 576.3, and 685.5 cm^{-1} modes consist of C–C–C and C–H out-of-plane motions, while C–C–C bending motions on the two, consecutive end rings (carbons 7 through 12, Fig. 1 molecule 3) of the benz[a]anthracene skeleton are responsible for the 621.2 cm^{-1} mode. The 650.2 cm^{-1} mode consists of C–C–C rocking motions of most of the PAH skeleton with the exception of the 7 and 8 groups on the skeleton. The 747.2 cm^{-1} mode, normally ascribed to the quartet hydrogens, is actually a mixture of the in-phase CH_{oop} motion of both quartet groups, which are out-of-phase with the CH_{oop} motion of the solo hydrogen (12) in the bay region and the duo hydrogen in the 5 position (Fig. 1 molecule 3). The 782.7 cm^{-1} mode is the result of C–C–C and C–H out-of-plane motions involving most, but not all, of the atoms in the molecule. The 805.4 cm^{-1} mode, traditionally called the "duo" hydrogen CH_{oop}, consists of the duo hydrogen CH_{oop} coupled most strongly, in-phase, with the quartet hydrogens (positions 1, 2, and 3) on the additional benzene ring and strongly coupled, out-of-phase, to the adjacent solo hydrogen (position 7). There is only slight coupling to the other hydrogen motions. While the 882.8 cm^{-1} mode is primarily due to solo CH_{oop} motion of both solo hydrogen atoms (7 and 12), they are slightly coupled, in-phase, to the duo hydrogens (5 and 6) and moderately coupled to the quartet hydrogen at position 10. The 944.3 cm^{-1} is primarily due to an anti-symmetric CH_{oop} motion of the quartet hydrogens (1, 2, 3, and 4), while the 951.9 cm^{-1} is a similar motion, but for the quartet hydrogens at positions 8, 9, 10, and 11.

Upon addition of a second benzene ring, forming dibenz[a,j]anthracene, the 450 to 725 cm^{-1} spectral region resembles that of the benz[a]anthracene, although the bands are shifted to different frequencies (see Fig. 4). The 493.1 cm^{-1} mode can best be described as an in-plane rocking of the central aromatic ring (carbon and hydrogen atoms) with corresponding distortions in the surrounding rings. In this molecule the 556.2 and 709.6 cm^{-1} modes consist of C–C–C and C–H out-of-plane bending motions, while the 591.9 and 648.8 cm^{-1} modes are in-plane C–C stretches.

The dibenz[a,j]anthracene shows one of the few serious disagreements between theory and experiment. Theory has a strong band at 847.9 cm^{-1} with an intensity of 29.3 km/mol that is solo H(14) out-of-plane bend. Using the 4–31G or cc-pVTZ basis set does not eliminate the problem, these basis sets simply shift to higher frequency 872.3 and 871.4 cm^{-1}, respectively. We note however, that while the 4–31G has essentially the same intensity (27.6 km/mol) as the 6–31G(d) basis set, the cc-pVTZ set has a smaller intensity (14.6 km/mol). There are weak bands in experiment at 861.6 and 879.8 cm^{-1}. This suggests that this is either a very rare example of where theory obtains a very poor intensity or the band intensity found in our matrix experiment has a much smaller intensity that would be seen in a gas-phase experiment.

It is interesting to note a gradual blue shift of the "solo" CH_{oop} mode with the addition of the benzene groups. The mode shifts

from 878.3 cm^{-1} in anthracene, to 882.8 cm^{-1} in benz[a]anthracene to 889.3 cm^{-1} in dibenz[a,j]anthracene. Similarly, the addition of a benzene ring shifts the "quartet" mode to the blue as well, but only with the first ring. The addition of the second benzene ring splits the motion of the solo hydrogen atoms (positions 14 and 7 in Fig. 1 molecule 8, dibenz[a,j]anthracene), with the solo hydrogen

Table 2
Summary of benz[a]anthracene and 1- and 2-azabenz[a]anthracene results. The intensities, A, are in km/mol and the band positions are in cm^{-1}. The theoretical results are taken from the B3LYP/6–31G(d) approach. For 1- and 2-azabenz[a]anthracene these results supersede our previous work.

benz[a]anthracene					1-azabenz[a]anthracene					2-azabenz[a]anthracene				
Experimental		Theory			Experimental		Theory			Experimental		Theory		
Center	A	Center	A	Sym	Center	A	Center	A	Sym	Center	A	Center	A	Sym
539.1	3.7	545.2	3.1	a″			480.7	8.4	a″			474.3	8.0	a″
576.5	4.0	577.0	5.0	a′	576.3	8.6	576.5	8.0	a′	513.9	10.8	521.2	5.1	a″
621.2	1.5	625.1	2.3	a′	619.9	1.9	623.7	2.2	a′	527.5	2.7	527.9	2.2	a′
650.2	3.7	651.5	4.3	a′	646.3	6.9	647.3	5.1	a′	576.1	11.7	580.6	8.0	a″
685.5	4.0	688.6	3.1	a″	694.4	11.4	699.7	8.4	a″	583.6	4.3	583.5	3.8	a′
737.4	2.8	742.4	1.1	a″	724.9	1.7	724.0	1.4	a′	621.7	2.1	625.5	2.5	a′
747.2	60.0	749.9	55.6	a″	741.4*	35.2	748.2	26.3	a″	638.4	1.1			
782.7	4.4	784.7	6.9	a″	761.9	1.0	763.9	1.7	a″	667.5	4.8	669.1	5.9	a′
805.4	18.8	810.7	13.7	a″	767.2	1.6	769.8	1.4	a′	741.3*	45.6	746.9	31.8	a″
876.1	2.2				773.2*	20.7	779.4	16.1	a″	767.9	8.5	765.0	8.7	a′
882.8	35.1	870.7	45.9	a″	794.4	2.0	792.6	2.1	a′	795.3*	2.7	803.0	1.4	a″
		873.7	3.0	a′	804.0*	23.9	810.8	16.7	a″	838.3	12.7	845.3	8.9	a″
888.3	6.7	896.8	7.4	a″	825.8*	9.1	834.0	6.3	a″	845.1	16.5	850.5	4.1	a″
		926.6	3.4	a″	844.2	5.3	851.9	5.9	a″	883.7*	59.1	878.3	58.3	a″
944.3	1.3	940.5	4.2	a″			881.7	6.2	a′	889.8*	11.0	880.9	2.3	a′
951.9	3.3	956.7	0.0	a″	884.4	41.8	886.7	36.7	a″	905.0	1.1	899.0	4.8	a″
1010.6	1.9	1025.2	2.2	a′	914.3*	11.8	929.5	2.5	a″	909.9	2.2	902.3	3.5	a′
1040.6	3.5	1054.1	3.2	a′	921.5	1.5				953.0	3.3	942.9	3.4	a′
1134.0	3.4	1130.4	1.6	a′	954.1	5.6	948.6	10.2	a″	982.2*	5.2	981.0	3.9	a′
1142.3	2.4	1147.8	0.9	a′	1009.9	2.7	1024.5	1.9	a′	1011.2	2.8	1025.6	1.8	a′
1156.0	3.7	1156.6	1.3	a′	1057.7	1.2				1059.3	4.4	1074.0	3.4	a′
1174.4	1.9	1175.6	2.2	a′	1099.9*	3.0	1095.4	2.5	a′	1132.5	2.6			
1240.6	4.6	1236.8	9.2	a′	1133.6*	7.4	1129.3	3.1	a′	1136.9	3.9	1139.2	1.4	a′
1276.6	3.5	1277.5	2.1	a′			1142.6	3.2	a′	1142.4	2.5	1149.0	3.2	a′
1281.2	3.4				1150.3	10.3	1153.6	6.5	a′	1166.3	2.4	1170.3	2.5	a′
1299.8*	2.9	1293.3	1.2	a′	1172.3	3.3	1169.4	3.4	a′	1179.7	2.4	1180.9	1.3	a′
1303.0					1211.3	1.5	1199.5	1.4	a′	1217.8	2.6	1222.1	2.4	a′
1310.0	4.4				1227.5*	2.1	1225.3	2.0	a′	1226.1	2.5			
1341.2	2.3	1344.2	4.6	a′	1254.8	0.8	1259.1	2.8	a′	1239.7*	23.8	1239.2	22.8	a′
1361.8	1.2	1362.5	2.5	a′	1269.6	5.3	1265.1	4.9	a′	1250.1	2.9			
1459.4	3.8	1460.0	6.7	a′	1279.9	2.1				1258.9	1.6			
1478.1	2.0				1287.4	2.6	1294.9	4.0	a′	1277.4	2.4	1278.3	1.6	a′
1483.7	1.4	1487.8	2.3	a′	1310.5	5.3	1306.6	3.7	a′	1285.5	4.5	1296.6	2.7	a′
1505.0	11.2	1507.4	14.8	a′	1340.0	2.6	1342.7	4.6	a′	1301.7*	2.2	1313.4	1.5	a′
1552.6	0.7	1558.8	2.3	a′	1415.9*	57.3	1405.0	48.6	a′	1342.0	3.2	1340.9	4.1	a′
		1637.6	2.5	a′	1440.9	14.6	1442.9	15.0	a′	1348.9	1.0			
2985.0	168.7	3042.2	6.0	a′	1451.2	5.0	1447.7	4.0	a′	1359.8	1.5			
3017.0		3045.9	0.8	a′	1478.8	2.0				1363.7	1.5	1363.1	4.0	a′
3044.0		3046.5	8.9	a′	1486.5	1.9	1488.0	2.7	a′	1374.6	1.7			
3065.0*		3048.6	3.5	a′	1493.5	11.2	1494.8	14.2	a′	1379.5	1.2			
3078.0		3050.8	1.8	a′	1543.4	21.3	1546.9	18.5	a′	1393.9	1.4	1391.7	1.2	a′
		3057.7	8.0	a′	1563.8	4.6	1566.0	2.6	a′	1408.3	4.9	1408.7	2.9	a′
		3063.9	9.8	a′	1601.7	4.1	1592.3	10.9	a′	1434.2	1.8			

Table 2 (*continued*)

benz[a]anthracene					1-azabenz[a]anthracene					2-azabenz[a]anthracene				
Experimental		Theory			Experimental		Theory			Experimental		Theory		
Center	A	Center	A	Sym	Center	A	Center	A	Sym	Center	A	Center	A	Sym
		3064.7	59.1	a'			1606.6	7.4	a'	1451.0*	17.1	1442.5	11.1	a'
		3066.2	14.8	a'			1629.0	8.5	a'	1476.5*	4.1	1452.4	9.8	a'
		3074.7	28.8	a'			1635.9	2.4	a'	1496.1	2.3	1485.3	2.9	a'
		3076.6	45.8	a'			3034.9	29.9	a'	1502.4	0.9	1503.6	7.2	a'
		3087.5	23.5	a'			3042.2	5.1	a'	1532.7	1.3	1537.4	2.4	a'
					3018		3047.0	7.8	a'	1586.4	3.6	1566.1	1.8	a'
					3052*		3051.8	11.9	a'	1589.4	6.7	1593.6	25.9	a'
					3059*	116.2	3063.4	25.2	a'	1606*	33.8	1609.1	24.2	a'
					3067*		3064.0	45.2	a'			1629.0	4.8	a'
					3089		3075.9	43.5	a'			1637.1	6.8	a'
							3079.5	30.1	a'			3044.1	5.3	a'
							3085.1	1.7	a'	3042.7		3045.2	23.4	a'
										3071.2*	88.2	3047.5	11.5	a'
										3083.4		3048.7	2.9	a'
												3050.0	4.3	a'
												3053.0	1.6	a'
												3065.7	22.0	a'
												3065.9	27.3	a'
												3068.8	50.6	a'
												3075.5	14.1	a'
												3078.3	37.1	a'

[a] b indicates a broad band, sh indicates a shoulder, while a * indicates the band is part of a complex.

in the bay region (14) being primarily responsible for the "solo" mode, occurring at 889.3 cm^{-1}. The "external" solo hydrogen at position 7 coupled strongly out-of-phase for the "duo" hydrogen mode. Although the "quartet" mode is somewhat coupled to most of the other hydrogen atoms in the molecule, it is most strongly coupled, in-phase, to the solo hydrogen atom in the bay region (position 14). Given the coupling of the quartet and solo hydrogens this may explain the successive shifts to the blue of the "solo" modes as well as the shift of the "quartet" modes. Although the "duo" hydrogens are coupled to both the solo and quartet hydrogen motions, the addition of another benzene ring does not appear to impact the position of the band.

Although the parent molecules dibenz[a,c]anthracene and dibenz[a,h]anthracene were not included in the experimental study, the theoretical data provides an interesting comparison. Dibenz[a,h]anthracene and dibenz[a,j]anthracene have very similar structures containing a bay solo, additional benzene rings and duo hydrogens. The major difference is the non-bay solo hydrogen in dibenz[a,j]anthracene. This is reflected in their spectra where the "quartet" and "duo" bands are quite similar, with the dibenz[a,h]anthracene "duo" modes shifted slightly to the blue. However, the solo region for dibenz[a,j]anthracene is much more complex, given the bay and non-bay solo hydrogens, than the purely "solo" bay hydrogens of dibenz[a,h]anthracene. Dibenz[a,c]anthracene is interesting in that it contains three sets of "quartet" hydrogens, two of which are equivalent, only bay "solo" hydrogens, and no "duo" hydrogens. The equivalent sets of "quartet" hydrogens, which form the bay regions, occur at a higher frequency than the "quartet" hydrogens on the anthracene structure. For dibenz[a,c]anthracene using the 6–31G(d) basis set, the solo hydrogens couple with the quartet hydrogens and split into two bands with similar intensity, one at 842 and the other at 862 cm^{-1}. This strong coupling does not occur for the cc-pVTZ basis set and only a single "solo" band is present at 876 cm^{-1}. The solid phase spectra on the NIST website appears more consistent with the cc-pVTZ result of a weak peak near 865 cm^{-1} and very strong peak near 888 cm^{-1}. However, there is no strong coupling of the solo and quartet hydrogens in dibenz[a,j]anthracene for any of the basis sets, so the dibenz[a,c]anthracene results do not shed any light on the difference between theory and experiment noted above for the dibenz[a,j]anthracene.

3.1.2. Nitrogen's Impact on the CH_{oop} Region(450 to 1000 cm^{-1})

Although previous papers have reported the spectra of anthracene and acridine [28–30], it is important to study the effect of replacing one of the anthracene CH groups with a nitrogen atom on the overall spectrum. Fig. 2 compares the anthracene and acridine spectra for the 500 to 1000 cm^{-1} region of these molecules. It is interesting to note that the bands visible at 469.7 and 601.6 cm^{-1} in acridine resemble the corresponding modes in anthracene. The presence of the nitrogen atom seems to have very little, if any, influence on these skeletal motions. The weak 523.6 cm^{-1} band visible in the spectrum of acridine resembles the rocking mode at 493.5 cm^{-1} of the central aromatic ring in dibenz[a,j]anthracene. The 618.1 cm^{-1} mode resembles the symmetric breathing modes of the two end rings, out-of-phase, with the breathing mode of the central ring. The 655.6 cm^{-1} mode is the result of CH–CH–CH in-plane rocking motions. The "quartet" mode, visible as a split band centered around 737 cm^{-1}, is identical to the motion in anthracene, although shifted higher in frequency by ≈10 cm^{-1}. Nitrogen's presence and position in acridine splits the "solo" mode. Shifting the "solo" motion involving hydrogen (10) and hydrogens 1, 9 (out-of-phase) and 3, 4 and 7, 6 (in-phase) down to 854.4 cm^{-1} and the "solo" motion coupled, in-phase, to hydrogens 2 and 8 and out-of-phase to hydrogens 6 and 4 (Fig. 1, molecule 1) up to 906.8 cm^{-1}. The modes at 958.2 and 921.7 cm^{-1} are similar to those at 957.2 and 908.7 cm^{-1} in anthracene. The new bands at 788.6 and 854.4 cm^{-1} arise from C–C

and C–H out-of-plane motions, while the 815.1 cm^{-1} band is the result of C–C stretches on both sides of the central ring. It appears that the presence of a nitrogen atom increases the intensity of the skeletal modes in this region in a fashion similar [27] to that for the C–C and C–H in-plane region.

Table 3
Summary of benz[a] and benz[c]acridine results. The intensities, A, are in km/mol and the band positions are in cm^{-1}. The theoretical results are taken from the B3LYP/6–31G(d) approach.

benz[c]acridine					benz[a]acridine				
Experimental		Theory			Experimental		Theory		
Center[a]	A	Center	A	Sym	Center	A	Center	A	Sym
		457.1	2.6	a′	458.9	0.8	458.8	2.0	a′
474.7	3.3	480.2	1.6	a″	492.3	3.0	491.3	2.8	a′
547.6	4.9	553.3	3.3	a″	542.5	7.4	548.6	7.2	a″
					569.9sh }	7.4			
575.3	6.1	575.4	1.4	a′	576.4* }		576.9	7.6	a′
		579.6	4.9	a″	618.1	3.4	620.5	4.3	a′
614.3	4.6	617.4	4.9	a′	651.6	4.1	652.4	5.1	a′
653.0	6.0	654.0	6.4	a′	753.6	78.1	757.1	69.9	a″
694.4	9.5	699.3	6.3	a″	792.7	1.0	794.6	2.3	a″
744.3	3.0	750.7	2.9	a″	833.1* }		837.3	26.8	a″
					834.8sh }	32.8			
					839.1sh }				
752.9	47.3	759.8	40.4	a″	857.6	7.6	862.9	7.5	a″
763.6	4.3	762.4	4.6	a′	867.1	1.9	870.5	5.6	a″
772.3	28.7	773.6	31.8	a″	874.9* }		872.1	3.7	a′
					876.3sh }	3.7			
					878.4sh }				
					903.8 }				
					905.9* }				
801.5	16.3	808.2	13.3	a″	}	11.6	904.3	12.6	a″
					908.6 }				
					912.3 }				
817.6	4.3	823.7	8.3	a″	946.2	1.3	930.2	5.2	a″
856.3	6.8	862.5	5.1	a″	955.9	1.4	949.0	3.6	a″
880.6	6.3	877.5	4.9	a′	983.9	3.3	981.5	3.1	a′
909.0	19.9	915.4	22.4	a″	1007.8* }				
					1010.3sh }	2.6			
955.9	4.2	949.3	6.3	a″	1025.1	0.3	1020.8	2.3	a′
1002.9	2.1	1007.0	4.2	a′	1041.1* }		1053.7	2.8	a′
					1043.9sh }	3.0			
1013.0	10.2	1022.4	5.4	a′	1126.8	4.1	1127.4	4.5	a′
1037.7	1.3	1047.5	2.4	a′	1138.3b	6.4	1139.8	3.4	a′
1131.5 }									
1134.0* }	5.6	1129.0	3.9	a′	1191.4b	3.1	1193.4	2.4	a′
1173.9	3.1	1177.0	3.4	a′	1219.2b	3.6	1217.3	2.3	a′
1228.7	1.8	1226.7	2.6	a′	1233.9* }		1239.0	7.0	a′
1299.3sh }					1238.3sh }	3.3			
1301.2* }	4.5	1298.9	6.8	a′	1248.1	2.4			
1304.3 }									
1309.7	5.0	1320.7	7.8	a′			1271.9	2.4	a′
1384.0	13.0	1374.2	15.2	a′	1315.0	2.5	1321.5	1.0	a′
1403.1	2.7				1321.6	0.6	1329.2	3.3	a′
1417.1	20.0	1407.3	16.5	a′	1348.4	7.2	1346.7	11.4	a′
		1418.7	3.0	a′	1375.4	4.5			
1453.5vb	4.6	1451.4	1.1	a′	1383.8	7.9			
					1407.0 }				
1479.3	7.4	1458.3	6.2	a′	1411.1* }	8.2	1373.8	9.9	a′
1485.1	2.9	1485.7	2.8	a′	1417.8	7.0	1403.4	7.6	a′
1496.6	30.0	1497.7	33.5	a′			1412.4	3.9	a′
1539.7	12.5	1541.4	17.5	a′	1459.5	2.7	1458.9	4.2	a′
1568.5* }		1566.1	5.6	a′	1476.6	7.1	1484.2	5.9	a′
1572.9 }	4.1								
1587.2	9.0	1593.4	18.1	a′	1506.6	22.6	1507.6	23.4	a′
		1618.4	7.9	a′	1516.7	2.2			

Table 3 (*continued*)

benz[c]acridine					benz[a]acridine				
Experimental		Theory			Experimental		Theory		
Center	A	Center	A	Sym	Center	A	Center	A	Sym
1622.3[b]	6.3	1620.7	1.4	a′	1543.3	10.1	1545.1	15.9	a′
		1637.7	5.6	a′	1567.6	2.9	1564.6	4.8	a′
3032.9 }		3042.4	6.2	a′			1592.1	11.7	a′
3048.7 }		3046.0	3.3	a′			1617.9	9.9	a′
3062.1* }	67.8	3048.5	3.4	a′	1620.5	11.9	1622.2	13.1	a′
3077.5 }		3048.8	6.3	a′			1635.8	1.3	a′
3087.9 }		3059.8	11.5	a′	3015.6 }		3047.4	2.9	a′
		3060.0	10.9	a′	3041.8 }		3049.3	0.7	a′
		3064.5	43.8	a′	3053.8 }		3053.4	10.3	a′
3109.0	1.6	3074.0	62.0	a′	3068.6* }	69.0	3058.0	12.0	a′
		3074.3	12.6	a′	3075.8 }		3059.9	13.8	a′
		3086.6	18.5	a′	3084.0 }		3063.9	6.5	a′
		3099.2	6.3	a′	3096.0 }		3074.5	9.1	a′
					3111.2 }		3074.9	52.3	a′
					3198.0	1.2	3084.0	29.7	a′
							3087.7	20.0	a′
							3089.1	10.3	a′

[a] vb indicates a very broad band, sh indicates a shoulder, while a * indicates the band is part of a complex.
[b] May suffer from a water contaminant.

Fig. 3 displays the 500 to 1000 cm^{-1} spectra for the various nitrogen substituted benz[a]anthracene molecules. The theoretical and experimental data for benz[a]acridine and benz[c]acridine can be found in Table 3. The results for 1 and 2-azabenz[a]anthracene were previously published [27]. The 450 to 700 cm^{-1} skeletal region is intriguing given the similar pattern displayed by all 5 molecules. Benz[a]anthracene along with benz[a] and benz[c]acridine all contain a vibrational mode around 652±2 cm^{-1}. 1- and 2-azabenz[a]anthracene exhibit a band significantly shifted from this position at 646.3 and 667.6 cm^{-1}, respectively. This confirms what we noted with theory earlier, that the additional benzene ring is heavily involved in the 652 cm^{-1} mode. However benz[a]anthracene, as well as 1- and 2-azabenz[a]anthracene all contain a mode around 621.8±0.8 cm^{-1}, while this band falls at 618.1 and 614.3 cm^{-1} in benz[a]acridine and benz[c]acridine, respectively. This indicates that the mode is tied more closely to the anthracene skeleton than the additional benzene ring. Indeed, theory confirms that this mode is the result of C–C–C scissoring motion on the two end rings of the anthracene moiety (positions 7–12, Fig. 1 benz[a]anthracene), with very minimal nitrogen involvement. Finally, all the molecules in this grouping have a band around 576.4±0.5 cm^{-1}.

The infrared spectra of benz[a]anthracene, benz[a] and benz[c] acridine all contain two inequivalent sets of "quartet" hydrogen atoms (positions 1–4 and 8–11). The quartets on the pendent benzene ring (positions 1–4) are broken up by a nitrogen atom for 1- and 2-azabenz[a]anthracene. As previously discussed, the "quartet" mode at 747.2 cm^{-1} in benz[a]anthracene is a mixture of duo, solo, and quartet hydrogen atom motions. This may help explain the observed trends for this band. For benz[a] and benz[c] acridine the mode shifts ≈6 cm^{-1} higher in frequency. For 1-azabenz[a]anthracene the band shifts ≈5 cm^{-1} lower in energy and its intensity is halved. The lower intensity is not simply the result of halving the number of quartet hydrogens in the molecule. Our calculations indicate that this mode, although still primarily "quartet" in nature is now coupled, slightly, in-phase with the duo hydrogens and coupled, slightly, out-of-phase with the trio hydrogen group on the pendent benzene ring. While the quartet hydrogens were coupled out-of-phase with the solo hydrogen atom in the bay region for the non-nitrogenated species, it is

mostly coupled, out-of-phase, to the solo hydrogen external to the bay region in 1-azabenz[a]anthracene (position 7, molecule 3, Fig. 1). This is likely due to hydrogen bonding occurring between the bay region solo hydrogen and the nitrogen atom. However, for the 2-azabenz[a]anthracene, the position of the nitrogen atom creates a second duo group, and a third solo hydrogen. In this instance the original duo hydrogen group is coupled, in-phase, with the quartet hydrogens, whereas the newly created duo and solo hydrogen atoms exhibit little involvement in this motion. Both of the solo hydrogens (positions 7 and 12, molecule 3, Fig. 1) on the anthracene structure are coupled out-of-phase with the quartet hydrogen atoms.

The 750 to 900 cm^{-1} region of this subset of molecules appears to present a very complex situation (see Fig. 3). However, some observations can still be made. All of the species have a band at about 750 cm^{-1} that arises from the symmetric out-of-plane bend of the quartet hydrogens; for many of the species the solo hydrogens move out-of-phase with the quartet hydrogens. The spectra differ in the presence of a second band at higher frequency. The medium sized

Table 4
Summary of dibenz[a,j]anthracene, dibenz[a,j]acridine, and dibenz[c,h]acridine results. The intensities, A, are in km/mol and the band positions are in cm^{-1}. The theoretical results are taken from the B3LYP/6–31G(d) approach.

dibenz[a,j]anthracene					dibenz[a,j]acridine					dibenz[c,h]acridine				
Experimental		Theory			Experimental		Theory			Experimental		Theory		
Center[a]	A	Center	A	Sym	Center	A	Center	A	Sym	Center	A	Center	A	Sym
493.1	2.3	493.2	2.4	b_2	516.5	7.5	492.8	8.0	b_2	568.1	11.5	571.4	8.0	b_1
556.2	3.0	556.7	2.7	b_1	521.1	4.0	521.2	1.6	a_1	590.2	2.7	593.3	3.3	b_2
591.9	10.6	596.0	9.9	b_2			522.8	8.2	b_1	652.9	5.4	654.3	5.3	a_1
648.8	3.2	651.7	2.6	a_1	537.6	4.3	537.7	3.2	b_2	710.8	2.3	709.7	1.6	a_1
710.4	7.5	710.5	7.1	b_1	592.3	8.0	595.7	10.2	b_2	719.6	15.1	723.1	10.6	b_1
740.1 / 743.2*	53.4	743.2	44.1	b_1	645.9	1.0	649.0	1.0	a_1	729.0	2.9	728.2	4.3	b_2
767.0	2.7	765.5	3.6	b_2	716.0	2.0	720.3	1.1	b_1	749.5	57.4	754.2	49.2	b_1
776.7	1.1	772.7	5.6	b_1	726.8	0.4	728.2	2.2	b_2	765.7	5.8	762.0	6.5	b_2
800.2sh / 801.7sh / 802.9*	46.2	803.3	44.5	b_1	747.5sh / 749.6	67.7	752.6	0.0	a_2	800.6	55.7	805.5	47.5	b_1
861.6	1.3	847.9	29.3	b_1			753.5	64.0	b_1	821.3	6.9	822.3	17.5	b_1
879.8	1.3	882.2	3.3	b_2	786.5	3.8	787.4	1.4	b_1	875.7	1.1	879.7	0.3	b_1
889.3	33.3	893.1	27.6	b_1	838.5	62.9	840.7	51.8	b_1	891.8	6.9	885.5	7.0	b_2
945.2	3.2	927.8	7.2	b_1			863.1	0.1	a_1	910.6	22.2	916.1	28.8	b_1
962.4	2.0	965.7	1.4	b_2	864.7	3.6	868.7	16.8	b_1	954.8	2.9	945.7	4.3	b_1
1037.6	3.0	1050.9	3.4	b_2	886.7	4.1	882.2	4.1	b_2	991.5	14.3	995.5	13.0	b_2
1047.2	4.3	1058.0	3.2	a_1	902.5* / 906.6sh	7.7	885.9	10.6	b_1	1014.6	2.9	1014.8	0.9	a_1
1172.4	3.9	1176.8	3.7	b_2	944.8	3.6	931.4	8.1	b_1	1038.7	4.1	1045.1	2.4	b_2
1213.3	2.6	1213.8	2.4	a_1	962.8	4.8	966.9	5.7	b_2			1046.7	4.5	a_1
1219.7	2.9	1223.3	12.0	a_1	1002.6	2.3	999.1	2.6	a_1	1112.1	3.8	1103.2	2.9	b_2
1226.3	10.5	1233.9	0.7	b_2	1038.0	2.3	1050.4	4.1	b_2	1145.8	2.9	1140.6	3.0	b_2
1269.3	5.0	1264.7	0.0	a_1	1106.2	4.0	1100.3	4.0	a_1	1156.4	0.9	1148.0	2.6	b_2
1283.0	2.9	1284.2	2.7	b_2	1192.1	6.7	1196.1	3.8	b_2	1175.3	4.4	1180.0	2.9	b_2
1334.6	2.0	1342.1	3.2	b_2	1214.9	6.7	1214.2	3.3	a_1	1215.5	3.4	1214.7	2.1	a_1
1352.7	4.1	1354.5	1.5	b_2	1219.4	2.3	1220.0	2.4	b_2	1222.4	3.0	1220.7	7.3	a_1
1430.4 / 1433.0*	14.6	1428.9	2.0	a_1	1224.1	4.9	1221.3	7.7	a_1	1269.0	2.4	1263.4	3.0	b_2
		1432.9	3.9	b_2	1279.6	1.6	1273.6	3.1	b_2	1315.6	1.6	1325.7	2.8	b_2
1458.3	17.1	1456.8	17.2	b_2	1307.3	1.1	1298.6	2.0	a_1	1335.8	4.2	1338.0	5.8	a_1
1498.2 / 1495.2*	14.3	1480.5	1.0	a_1	1325.0sh / 1328.9*	3.0	1332.2	2.5	a_1	1391.0	11.5	1386.3	41.4	b_2
		1498.5	14.6	b_2			1344.0	0.7	b_2	1400.3	44.1	1394.7	4.8	a_1
1518.9	12.3	1520.6	10.7	a_1	1379.7* / 1386.1sh	44.4	1374.6	58.2	b_2	1449.8	6.0	1443.2	8.0	a_1
1528.1	2.1						1384.4	0.1	a_1	1454.4	6.0	1453.3	10.2	b_2
1557.1	1.7	1560.4	2.1	b_2	1416.6	7.9	1416.6	4.1	b_2	1477.4	11.0	1478.4	9.6	a_1
		1634.9	2.6	a_1	1437.8	8.9	1430.3	8.7	a_1	1481.3	25.3	1483.7	33.5	b_2
3014.2	16.2				1457.7	5.1	1455.7	8.2	b_2	1513.4	14.8	1514.1	15.8	a_1

(continued on next page)

Table 4 (*continued*)

dibenz[a,j]anthracene					dibenz[a,j]acridine					dibenz[c,h]acridine				
Experimental		Theory			Experimental		Theory			Experimental		Theory		
Center[a]	A	Center	A	Sym	Center	A	Center	A	Sym	Center	A	Center	A	Sym
3044.7*	141.6	3042.2	7.2	a_1	1487.9	26.7				1548.7*	7.3	1546.4	7.9	b_2
3061.8		3045.8	0.3	b_2	1492.2*		1494.1	33.1	b_2	1569.9[a]	3.5	1567.8	3.8	a_1
3092.5		3046.7	8.4	a_1	1495.4					1576.9	3.1	1594.8	25.2	b_2
3118.5		3048.8	8.1	b_2	1527.6	1.3	1525.6	3.4	a_1	1635.0	6.3	1634.9	6.5	a_1
3128.9		3049.0	0.1	a_1	1548.8vb	8.6	1552.5	10.6	b_2	3016.6	123.8	3042.3	7.0	a_1
		3058.0	10.3	a_1	1575.3	1.3	1567.6	3.8	a_1	3034.5		3045.8	0.5	b_2
		3058.3	3.2	b_2	1585.0	2.6	1589.4	16.1	b_2	3044.3		3046.6	11.2	a_1
		3064.7	24.4	b_2	1615.1	25.3	1615.7	24.2	b_2	3051.4		3048.7	3.5	b_2
		3065.3	61.1	a_1	3012.9	6.3	3048.2	0.3	a_1	3059.4*		3048.8	0.0	a_1
		3072.2	0.1	a_1	3043.6	87.6	3048.2	2.2	b_2	3078.8		3059.6	10.8	b_2
		3073.3	82.7	b_2	3049.0		3052.7	8.7	a_1	3102.6		3059.6	8.5	a_1
		3080.9	26.0	a_1	3061.6		3052.8	13.9	b_2			3064.3	32.5	b_2
		3084.3	1.4	b_2	3076.3*		3057.9	18.1	a_1			3064.8	60.4	a_1
		3108.5	14.3	a_1			3058.5	4.8	b_2			3074.1	67.2	b_2
							3069.9	1.1	a_1			3074.3	18.0	a_1
							3071.9	70.2	b_2			3100.5	0.7	b_2
							3078.8	24.7	a_1			3101.1	11.2	a_1
							3081.1	9.0	b_2					
							3087.8	12.0	b_2					
							3088.2	16.4	a_1					
							3097.8	17.8	a_1					

[a] vb indicates a very broad band, sh indicates a shoulder, while a * indicates the band is part of a complex.

band around 782.7 cm^{-1} in benz[a]anthracene shifts to lower energy and gains intensity in benz[c]acridine. This band also appears at lower energy for 1- and 2-azabenz[a]anthracene, but is weaker than for benz[c]acridine. It seems completely absent in benz[a]acridine. The theoretical spectra show that for benz[a]anthracene this mode is somewhat mixed in character; the largest motion is for hydrogens 3, 4, and 12 out-of-phase with hydrogen 1. The band in 1-azabenz[a]anthracene is similar, involving the in-phase motion of hydrogens 2, 3, and 4, which are out-of-phase with the motion of hydrogens 5 and 6. In benz[c]anthracene the mode is the in-phase motion of hydrogens 2, 3, 4, 8, and 9, which are out-phase with hydrogen 11. We also note a significant motion of the carbon(11) adjacent to the nitrogen. To our surprise the band in 2-azabenz[a]anthracene is totally different in character, being an in-plane motion. An inspection of all the modes in this region for all of the species shows several bands involving out-of-plane quartet modes and some in-plane modes. It appears that the addition of the nitrogen can enhance or suppress the intensity of bands in this region.

The "duo" mode at 805.4 cm^{-1} in benz[a]anthracene shifts slightly to the red (1–3 cm^{-1}) in benz[c]acridine and 1-azabenz[a]anthracene, but appears to shift significantly to the blue (≈30 cm^{-1}) and increases in intensity for the 2-azabenz[a]anthracene and benz[a]acridine. In the unsubstituted species (benz[a]anthracene), this "duo" CH_{oop} motion is strongly coupled out-of-phase with the adjacent solo hydrogen (position 7), moderately coupled, in-phase, to hydrogen positions 1, 2, and 3, and slightly coupled out-of-phase with the quartet hydrogens 4, 11, and 10. Given its strong out-of-phase coupling to the adjacent solo hydrogen, it is not surprising that replacement of the CH solo with a nitrogen atom in benz[a]acridine causes such a drastic shift in the "duo" band position. An inspection of the theoretical 2-azabenz[a]anthracene spectrum shows that the "duo" mode is actually shifted about 7 cm^{-1} to the red and is weak, while the bands observed at 838 and 845 cm^{-1} are modes that are composed mostly of quartet and/or motions of hydrogens on the ring with the nitrogen. We should note that these modes contain some motion of the duo hydrogens, but not as much as the band near 800 cm^{-1}.

The position and intensity of the "solo" hydrogen mode for 1- and 2-azabenz[a]anthracene closely resembles that of their unsubstituted parent molecule (882.8 cm^{-1}) although both are slightly higher in frequency. However, this is decidedly different for benz[a] and benz[c]acridine. In benz[c]acridine, the solo mode shifts ≈26 cm^{-1} higher in energy and has a smaller intensity. The intensity reduction is consistent with one few solo hydrogen atoms than in the parent. Although a similar shift is observed in benz[a]acridine, the "solo" bands intensity is significantly diminished. The origin of this larger reduction in intensity for benz[a]acridine is not obvious from the modes. For both benz[a]acridine and benz[c]acridine, the mode is mostly solo in origin, but some other motions also contribute, and these contributions are different for the two positions of the nitrogen atom. That is the nitrogen position affects the non-solo component of the mode and thus affect the intensity much more than its position.

The dibenz series of molecules are shown in Figs. 4 and 5, with the experimental and theoretical data provided in Tables 4 and 5. As with the benz[a]anthracene series of molecules, the 450 to 725 cm^{-1} region contains the series of sharp, weak to medium strength bands resulting from the skeletal motions described earlier. It is interesting to note that dibenz[a,j]anthracene and dibenz[a,j]acridine exhibit very similar bands around 557, 592, 646, and 707.5 cm^{-1}, indicating the presence of nitrogen inside the bay region (position 14), formed by the two additional benzene rings, does not inhibit these skeletal motions. However, the bands occurring at 556.2, 648.8, and 709.6 cm^{-1} in dibenz[a,j]anthracene shift higher in energy to 568.1, 652.9, and 719.6 cm^{-1} for dibenz[c,h]acridine, while the 591.9 cm^{-1} appears essentially unchanged. We note that dibenz[c,h]acridine has a band at 710.8 cm^{-1}, which might indicate a much smaller shift, but this band is different in character from the symmetric duo band in

Table 5
Summary of dibenz[a,h]anthracene, dibenz[a,h]acridine, dibenz[a,c]anthracene, and dibenz[a,c]acridine results. The intensities, A, are in km/mol and the band positions are in cm^{-1}. The theoretical results are taken from the B3LYP/6–31G(d) approach.

dibenz[a,h]anthra			dibenz[a,h]acridine					dibenz[a,c]anthra			dibenz[a,c]acridine				
Theory			Experimental		Theory			Theory			Experimental		Theory		
Center[a]	A	Sym	Center	A	Center	A	Sym	Center	A	Sym	Center	A	Center	A	Sym
483.0	5.1	b_u	482.6	4.6	481.8	4.6	a'	469.5	7.2	b_1	468.9	4.7	475.0	2.2	a''
534.3	7.1	a_u	508.4	1.3	508.8	0.8	a'	552.4	3.5	b_1	550.6	4.9	549.8	0.1	a'
651.3	13.0	b_u	532.0	13.3	537.9	10.7	a''	578.4	10.6	a_1			555.4	3.7	a''
667.7	5.6	a_u	651.1	11.1	652.6	13.1	a'	622.7	4.3	b_2	575.7	7.6	577.1	10.2	a'
741.2	1.6	b_u	671.6	8.5	675.6	6.0	a''	713.4	28.0	b_1	618.7	3.4	621.8	5.0	a'
747.0	51.2	a_u	747.1*	50.7	752.0	42.9	a''	759.9	87.5	b_1	622.7	2.1	625.8	1.3	a'
769.1	4.7	b_u	751.4		757.4	4.2	a''	842.2	20.1	b_1	722.6	36.0	723.9	34.7	a''
807.6	40.4	a_u	771.1	3.8	768.7	6.1	a'	862.5	21.1	b_1	759.0	44.3	758.9	19.1	a''
864.7	4.1	a_u	802.8	4.9	807.9	5.4	a''	885.6	1.0	b_2	767.6	48.8	770.2	73.0	a''
869.0	54.6	a_u	812.7*	40.0	818.7	42.3	a''	923.0	2.1	b_1	802.3	4.4	800.3	3.9	a''
			816.9												
876.3	6.0	b_u	834.7*	28.2	836.5	18.7	a''	939.3	3.0	b_1	814.9	2.1	814.9	2.0	a'
			838.9												
928.6	8.7	a_u	866.3	2.0	869.5	6.5	a''	1002.4	1.4	b_2	856.3	5.7	861.5	4.7	a''
											902.4				
1026.9	2.1	b_u	878.2	8.0	874.9	5.8	a'	1033.7	2.7	a_1	904.5*	8.2	898.5	10.5	a''
											909.7				
1054.3	6.0	b_u	887.2	3.7	883.3	3.0	a'	1066.9	4.4	b_2			920.3	2.7	a''
1106.6	1.9	b_u	907.3	14.9	903.4	19.3	a''	1076.8	1.5	a_1	953.9	3.2	947.1	3.5	a''
											958.8				
1150.2	1.0	b_u			930.6	6.1	a''	1136.2	1.7	b_2	965.3	2.1	961.4	2.1	a'
1186.2	3.3	b_u	1016.9	2.4				1176.8	1.0	a_1	1008.1	2.0	1003.4	1.6	a'
1211.5	4.8	b_u	1025.5	14.7	1032.8	13.7	a'	1204.4	1.3	a_1	1038.2	11.7	1044.3	10.4	a'
			1108.0	3.8											
1223.4	10.9	b_u	1110.3		1103.1	3.7	a'	1204.8	1.2	b_2	1052.3	4.5	1063.0	4.6	a'
1295.7	1.2	b_u	1136.6	2.2	1140.6	1.6	a'	1233.0	5.7	b_2	1134.3	5.7	1131.1	5.9	a'
1330.5	5.0	b_u	1189.1	6.0	1193.9	4.0	a'	1258.7	4.1	a_1	1148.4	3.8	1151.6	1.8	a'
1352.4	2.9	b_u			1217.2	3.0	a'	1283.6	2.4	b_2	1201.5	3.4	1205.3	2.7	a'
			1218.9*	8.2											
1433.6	4.8	b_u	1223.8		1221.3	5.6	a'	1312.3	1.4	a_1	1245.3	0.9	1240.2	3.4	a'
1439.7	1.1	b_u	1231.0	1.2	1227.3	2.4	a'	1319.7	1.3	b_2	1261.9	2.6	1262.8	5.3	a'
1459.9	29.0	b_u	1262.3*	2.5	1260.2	3.2	a'	1348.1	2.2	b_2	1304.7	3.6	1296.0	6.3	a'
			1266.2								1304.7				
1514.8	14.3	b_u	1318.2	8.4				1359.0	2.1	a_1	1311.0*	6.2	1311.9	1.6	a'
1559.8	2.2	b_u	1321.7		1328.0	14.7	a'	1398.0	1.1	a_1	1314.9		1325.4	5.2	a'
											1342.4				
1618.2	3.2	b_u	1338.7	1.1	1339.5	0.0	a'	1434.1	18.6	a_1	1345.5	12.6	1345.3	8.3	a'
1629.8	1.4	b_u	1374.0	9.9	1371.7	16.0	a'	1439.3	5.9	b_2	1348.8*		1348.9	5.1	a'
											1377.7	25.4			
3045.0	1.1	b_u	1389.2	2.4				1453.5	2.4	a_1	1383.2*		1378.8	29.5	a'
3048.4	8.2	b_u	1403.1	49.5	1393.4	34.2	a'	1457.3	6.2	b_2	1391.5	9.2			
3057.0	15.4	b_u			1433.5	2.1	a'	1499.9	17.9	b_2	1398.9	2.7			
			1441.0sh	17.5							1406.5				
3063.4	54.6	b_u	1447.0		1442.6	10.9	a'	1516.5	17.5	a_1	1415.0	25.4	1410.6	30.3	a'
3064.9	29.6	b_u	1453.8	17.0	1456.5	23.4	a'	1605.4	1.6	b_2	1420.7		1444.8	2.9	a'
			1456.1								1443.7	15.9			
			1458.4*					3046.0	4.8	b_2	1449.0*		1447.7	12.0	a'

(continued on next page)

Table 5 (*continued*)

dibenz[a,h]anthra			dibenz[a,h]acridine					dibenz[a,c]anthra			dibenz[a,c]acridine				
Theory			Experimental		Theory			Theory			Experimental		Theory		
Center[a]	A	Sym	Center	A	Center	A	Sym	Center	A	Sym	Center	A	Center	A	Sym
3074.4	77.5	b_u	1500.2	11.1	1500.1	13.0	a'								
3085.9	55.1	b_u	1511.4*	18.7	1512.2	20.5	a'	3056.0	1.7	a_1	1463.6	4.1	1462.7	2.7	a'
			1514.8												
			1550.4	8.3	1550.1	7.7	a'	3063.7	23.9	b_2	1476.6	3.6	1477.3	1.6	a'
					1566.9	4.5	a'	3068.4	50.7	b_2	1495.5	12.8	1497.1	16.2	a'
					1592.9	22.4	a'	3070.1	27.7	a_1	1509.9	36.4	1508.9	36.3	a'
			1618.2	7.1	1616.5	10.7	a'	3076.2	32.7	a_1	1551.2	4.9	1553.7	9.6	a'
					1617.7	2.9	a'	3078.0	8.6	a_1			1572.0	4.2	a'
			3018.2	117.3	3045.3	1.2	a'	3099.4	43.8	b_2	1584.6	5.6	1585.8	2.4	a'
			3038.5		3048.5	1.7	a'	3099.9	11.6	a_1			1598.8	24.4	a'
			3046.7		3049.2	1.1	a'	3106.6	32.7	a_1	1627.5	6.7	1614.4	1.3	a'
			3061.5*		3053.7	9.2	a'				3038.9	89.0	3047.6	4.0	a'
			3080.7		3058.0	13.9	a'				3047.6		3054.7	2.5	a'
			3122.0	1.4	3059.7	8.4	a'				3065.1		3056.4	1.6	a'
					3063.2	29.6	a'				3083.3*		3059.9	9.1	a'
					3064.8	16.7	a'				3109.9		3066.6	28.6	a'
					3074.0	48.7	a'				3123.7		3070.1	30.2	a'
					3074.7	33.5	a'						3073.2	4.4	a'
					3084.1	31.5	a'						3074.4	33.7	a'
					3087.6	10.8	a'						3084.5	0.21	a'
					3099.1	7.1	a'						3086.6	22.0	a'
													3091.0	30.7	a'
													3102.1	33.7	a'
													3105.0	9.0	a'

[a] sh indicates a shoulder, while a * indicates the band is part of a complex.

dibenz[a,j]anthracene at 709.6 cm^{-1} or the dibenz[c,h]acridine band at 719.6 cm^{-1}.

Although structurally different, dibenz[a,h]acridine exhibits a band at 651.1 cm^{-1}, similar to that observed in the three previously discussed dibenz and benz[a]anthracene species. Indeed, our calculations reveal that this motion is the result C–C–C and C–N–C scissoring motions (bending). Dibenz[a,c]acridine is unique in that most of its bands in the 450 to 725 cm^{-1} region are shifted from those of the other dibenz species.

The CH_{oop} quartet region provides some interesting insight into the dibenz molecular structure. Dibenz[a,j]anthracene, dibenz[a,j]acridine, and dibenz[c,h]acridine exhibit identical structures with the exception of the presence and position of the nitrogen atom. The presence of the nitrogen atom shifts the CH_{oop}" quartet" mode (743.2 cm^{-1} in the parent) ≈6.5 cm^{-1} to the blue, but the nitrogen's position inside or outside (positions 7 or 14 in Fig. 1 dibenz[a,j]anthracene) the bay region does not seem to impact the band position, but may result in a slight increase in intensity for dibenz[a,j]acridine (see Table 4). The "quartet" mode in dibenz[a,h]acridine, positioned at 747.1 cm^{-1}, is similar to that of dibenz[a] and [c] acridines. One may recall from the earlier discussions that the "quartet" mode in the parent molecule is moderately coupled, in-phase, to the solo hydrogen external to the bay region at position 7 and out-of-phase with duo hydrogens at positions 5 and 9 (Fig. 1, molecule 8). Thus, nitrogen's position in these three acridines would not be expected to produce a drastic change in the "quartet" CH_{oop} modes.

Dibenz[a,c]acridine is interesting in that it contains three, inequivalent, sets of "quartet" hydrogen atoms, no "duo" hydrogen atoms, and only a single "solo" hydrogen atom. This produces three "quartet" bands at 722.6, 759.0, and 767.6 cm^{-1} (see Fig. 5). The band at 722.6 cm^{-1} is very similar in character to the band at 713 cm^{-1} (theory) in the parent, but the substitution of the nitrogen removed the solo–quartet coupling, which shifts the band to the blue. Since the solo motion was out-of-phase with the quartet motion, its removal also increases the intensity. The nitrogen splits symmetric band at 760 cm^{-1} (theory) in the parent into two bands, by separating the motion of hydrogens 1, 2, 3, and 4 from hydrogens 5, 6, 7, and 8, Fig. 1, molecule 13.

The CH_{oop}" duo" modes provide insight into the effect of the position of the nitrogen atom in the PANH structure on the IR spectra. For dibenz[a,j]anthracene the duo mode occurs at 802.9 cm^{-1} and a similar band is apparent at 800.6 cm^{-1} for dibenz[c,h]acridine. This would seem to indicate that the nitrogen atoms replacement of the CH solo group inside the bay region (position 14) has little influence on the "duo" mode's position, although the nitrogen does increase the modes intensity. As discussed above, our calculations indicate the "duo" hydrogens are coupled out-of-phase with the CH_{oop} motion of the external solo hydrogen (position 7, Fig. 1, molecule 8) with little, if any, coupling with the solo hydrogen in the bay region (position 14). Thus, when the nitrogen atom replaces the external solo hydrogen between the duo hydrogens, it alters the "duo" motion, causing an in-phase coupling of the duo hydrogens to the solo hydrogen in the bay region, which results in the "duo" mode shifting ≈35 cm^{-1} to the blue as well as an increase in intensity.

Dibenz[a,h]acridine contains two duo hydrogen groups, one next to the nitrogen atom and one on the opposite side of the PANH skeleton (molecule 12, Fig. 1). In the parent, there is one strong duo mode at 808 cm^{-1} (theory), which involves both duo and solo hydrogen motion. Substituting nitrogen for CH leads to three bands in

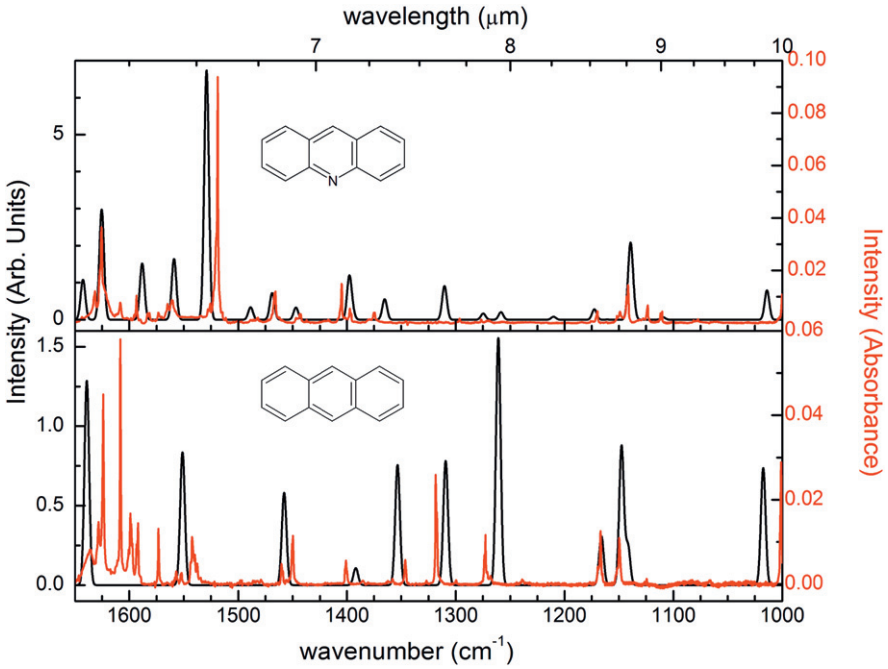

Fig. 6. The 1000–1650 cm^{-1} region of the experimental (shown in red) and theoretical (B3LYP/6–31G(d) and shown in black) spectra for anthracene and acridine. Experimental spectra have been normalized to 1×10^{16} molecules.

this region. The two stronger bands are shifted by ≈10 and 30 cm^{-1} to higher frequency, with the duo adjacent to the nitrogen being the higher of two. Nitrogen's presence also activates a previously IR inactive "duo" mode at 812.7 cm^{-1}, where the CH_{oop}" duo" hydrogen modes are out-of-phase with each other, but this band is quite weak.

Dibenz[a,j]anthracene exhibits its CH_{oop}" solo" motion around 889.3 cm^{-1}, ≈5 cm^{-1} higher in energy than benz[a]anthracene, with a small shoulder at 879.8 cm^{-1}. Our calculations reveal that the CH_{oop}" solo" mode is actually split for dibenz[a,j]anthracene. The lower frequency mode being primarily the result of the bay solo (position 14, Fig. 1, molecule 8) with very slight coupling, in-phase, to hydrogens 3, 5 through 9, and 11. The higher frequency solo mode is due to the solo hydrogen external to the bay region with moderate in-phase coupling to hydrogens 5 and 9 and slightly coupled, out-of-phase, to the solo hydrogen in the bay region. As noted for the benz[a]anthracene series, placement of the nitrogen atom in the external acridine position shifts the "solo" mode ≈20 cm^{-1} higher in

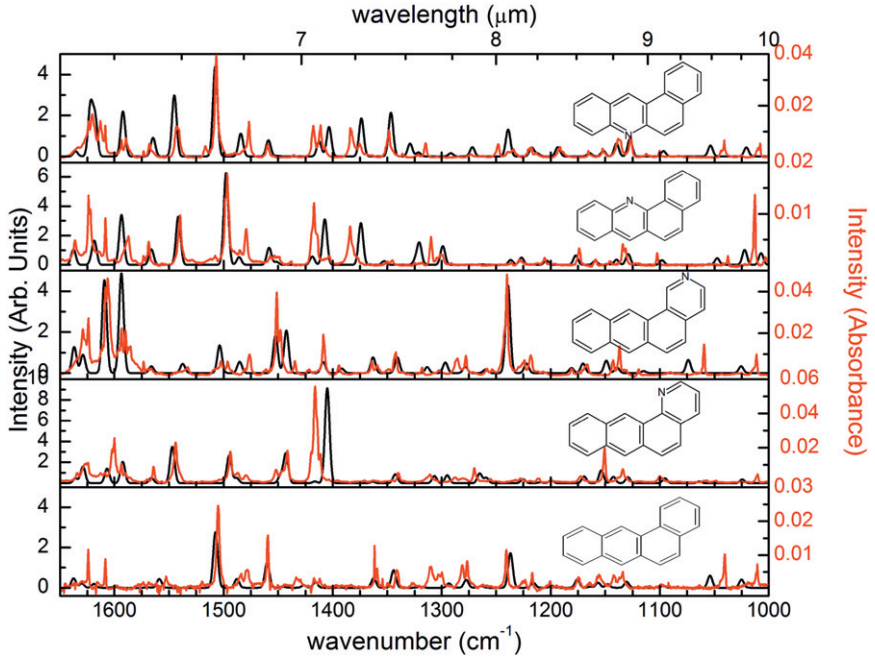

Fig. 7. The 1000–1650 cm^{-1} region of the experimental (shown in red) and theoretical (B3LYP/6–31G(d) and shown in black) spectra for the species derived from benz[a]anthracene. Experimental spectra have been normalized to 1×10^{16} molecules.

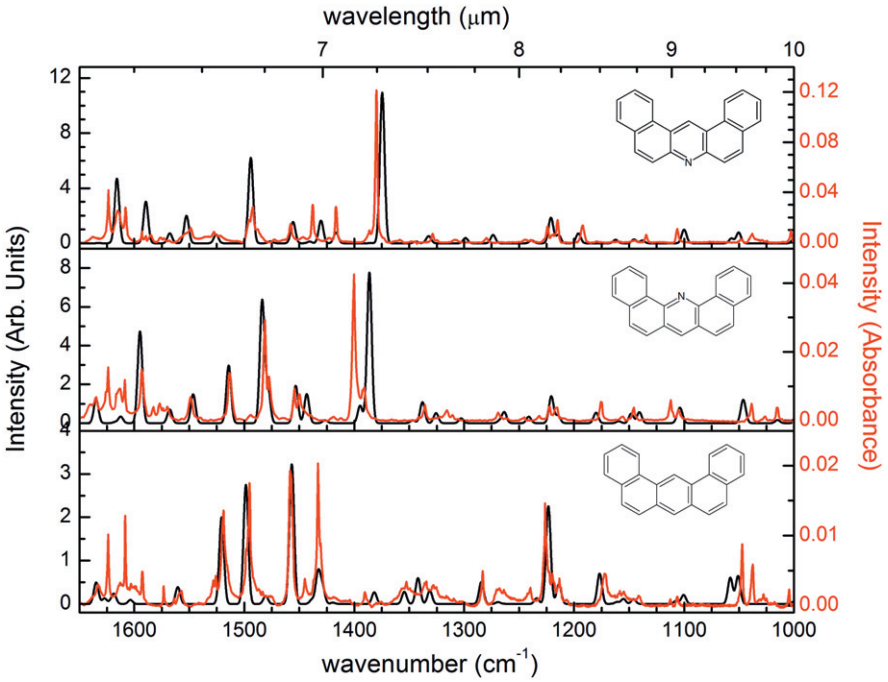

Fig. 8. The 1000–1650 cm^{-1} region of the experimental (shown in red) and theoretical (B3LYP/6–31G(d) and shown in black) spectra for the species derived from dibenz[a,j]anthracene. Experimental spectra have been normalized to 1×10^{16} molecules.

frequency than the non-nitrogenated parent or if the nitrogen was placed on a side ring.

It is interesting to note that for dibenz[a,j]acridine and dibenz[a,c]acridine and, to a lesser extent dibenz[a,h]acridine the intensity of the "solo" mode is weak to almost non-existent. This is similar to what was observed for the benz[a]acridine "solo" mode. As previously noted, the experimental results and the calculations show significant in-phase coupling between the duo hydrogen atom motions and of the external solo hydrogen atom (position 7). Replacing the solo CH group by a nitrogen atom naturally eliminates the one C–H solo stretch, but also seems to reduce the other solo band as well. The only exception to this is dibenz[a,h]acridine, where there are two solo–duo pairs so a solo–duo interaction remains even after substitution of a nitrogen for a CH group.

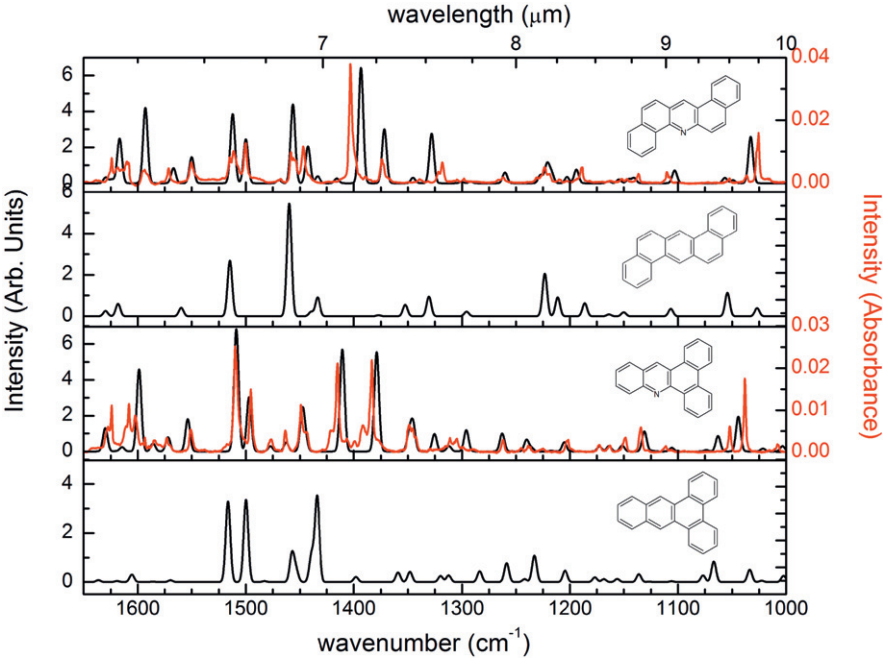

Fig. 9. The 1000–1650 cm^{-1} region of the experimental (shown in red) and theoretical (B3LYP/6–31G(d) and shown in black) spectra for the species derived from dibenz[a,h]anthracene and dibenz[a,c]anthracene. Experimental spectra have been normalized to 1×10^{16} molecules.

Some overall observations for this region of the spectra are: 1) Duo hydrogens next to a nitrogen atom experience a significant blue shift, while those further away show almost no effect. 2) For acridine, the N in the central ring induces two bands with a solo contribution. The addition of benzene rings hampers this coupling of the solo and quartet modes which reduces the intensity of the solo bands. 3) The quartet bands for benz[a]anthracene and benz[a]acridine are similar, but the addition of N to the pendent ring splits the quartet into solo, duo, and trios that leads to new bands that can be either blue or red shifted relative to original quartet bands depending on their interaction with the N atom.

3.2. The C–H and C–C In-Plane Region (1000 to 1650 cm^{-1})

The C–C and C–H in-plane region for the anthracene, benz[a]anthracene, and dibenzanthracene series of molecules are shown in Figs. 6 through 9. These results confirm the results in Mattioda et al. [27], which indicated that the presence of a single nitrogen atom increases the intensity of bands in the 1000 to 1600 cm^{-1} region over the non-nitrogenated species. This factor of 2 increase is similar, though less intense, to what is observed upon ionization of a PAH. The results of this investigation are provided in Table 6 and contain experimental and theoretical results for completeness. It is interesting to note that, regardless of the number of rings, the ratio of band intensities remain constant, that is the PANH to PAH ratio for the CH_{oop} regions is ≈1, the C–C and C–H in-plane region ratio is ≈2 and the C–H stretching ratio is slightly depressed ≈0.6 (experimental) and ≈0.8 (theoretical). However, in this study, we note that this increase in intensity is primarily the result of increased band intensity in a very narrow frequency range 1375 to 1600 cm^{-1}(see Table 6). The intensity of bands in this region exhibit a 2 to 6 fold increase (experimentally) and a 2 to 8 fold increase (theoretically) in intensity over their parent PAH species, with the position of the nitrogen atom impacting the increase in intensity (see the benz[a]anthracene series in Table 6). This increase in intensity over this limited spectroscopic region is also observed in the molecules of our previous study, with the possible exception of 2-azapyrene. The reason for this region's increase in intensity is discussed below.

The second item mentioned in Mattioda et al. [27] regarding the 1000–1600 cm^{-1} region and the presence of nitrogen in a PAH, is the appearance of an intense band around 1400 cm^{-1}, which was the result of a C–N–C rocking motion of the hydrogen atom para to the nitrogen. Indeed, in this study dibenz[a,j]acridine, dibenz[c,h]acridine, dibenz[a,h]acridine, and dibenz[a,c]acridine (Figs. 8 and 9 and Table 3) exhibit an intense band between 1370 and 1400 cm^{-1}, along with the 1-azabenz[a]anthracene discussed in Mattioda et al. [27] However, it is interesting to note that acridine, dibenz[a]acridine, and dibenz[c]acridine do not exhibit a similarly intense band in this area (see Figs. 6 and 7 as well as Tables 1 and 2). However, the acridine spectrum has a strong band at 1518.9 cm^{-1} and there seems to be a similar feature, although not as strong, in dibenz[a]acridine and dibenz[c]acridine. The other acridine molecules contain a feature in this region as well, although it is not as strong as in the previously mentioned species. An inspection of the mode shows that it is a C–N–C asymmetric stretch with a para hydrogen in-plane wag; it falls between ≈1480 and 1515 cm^{-1}. For 2-azabenz[a]anthracene, which does not have a hydrogen para to the nitrogen, there is a moderately strong band at 1451 cm^{-1} arising from the C–N–C asymmetric stretch. A closer inspection of the data reveals that some species have both bands, but one tends to be larger than the other, see for example dibenz[a,h]acridine where there is a strong band at 1403 cm^{-1} and a weaker band at about 1510 cm^{-1}.

Previously [27], we noted that 1-azachrysene did not contain an intense 1400 cm^{-1} feature found for other PANH molecules, however, it does contain an intense mode at 1478.6 cm^{-1}. In addition,

Table 6
The intensities for a PANH and its PAH parent broken down by frequency ranges and the ratio of the PANH intensities to those of the parent. The theoretical results are taken from the B3LYP/6–31G(d) approach.

	Experiment			Theory			Experiment		Theory	
	500–1100	1100–1600	2950–3150	500–1100	1100–1600	2950–3150	500–1375	1375–1600	500–1375	1375–1600
PAH (km/mol)										
Anthracene	134	37	97	135	32	178	157	13	160	8
Benz[a]anthracene	163	65	169	171	62	211	204	22	200	29
Dibenz[a,j]anthracene	181	106	158	200	84	248	221	66	232	53
Dibenz[a,h]anthracene				207	83	242			238	52
Dibenz[a,c]anthracene				194	95	239			219	70
PANH (km/mol)										
Acridine	132	103	72	148	91	139	154	81	172	67
1-azabenz[a]anthracene	197	166	132	162	156	170	241	122	201	116
2-azabenz[a]anthracene	213	113	86	164	99	177	280	46	207	55
Benz[a]acridine	177	113	71	178	129	168	215	76	220	88
Benz[c]acridine	189	135	69	186	154	185	218	107	221	120
Dibenz[a,j]acridine	211	160	94	209	179	199	242	129	241	148
Dibenz[c,h]acridine	224	173	124	219	200	232	255	143	258	161
Dibenz[a,h]acridine				218	203	213			280	141
Dibenz[a,c]acridine				205	223	210			256	172
Ratio PANH/PAH										
Acridine	0.99	2.78	0.74	1.10	2.84	0.78	0.98	6.23	1.08	8.38
1-azabenz[a]anthracene	1.21	2.55	0.78	0.95	2.52	0.81	1.18	5.55	1.01	4.00
2-azabenz[a]anthracene	1.31	1.74	0.51	0.96	1.60	0.84	1.37	2.09	1.04	1.90
Benz[a]acridine	1.09	1.74	0.42	1.04	2.08	0.80	1.05	3.45	1.10	3.03
Benz[c]acridine	1.16	2.08	0.41	1.09	2.48	0.88	1.07	4.86	1.11	5.55
Dibenz[a,j]acridine	1.17	1.51	0.59	1.05	2.13	0.80	1.10	1.95	1.04	2.79
Dibenz[c,h]acridine	1.24	1.63	0.78	1.10	2.38	0.94	1.15	2.17	1.11	3.04
Dibenz[a,h]acridine				1.05	2.45	0.88			1.17	2.01
Dibenz[a,c]acridine				1.06	2.35	0.88			1.28	2.01
Average	1.16	2.00	0.61	1.04	2.29	0.83	1.13	3.76	1.10	3.64
Standard deviation	0.10	0.49	0.17	0.05	0.35	0.05	0.13	1.79	0.08	2.12

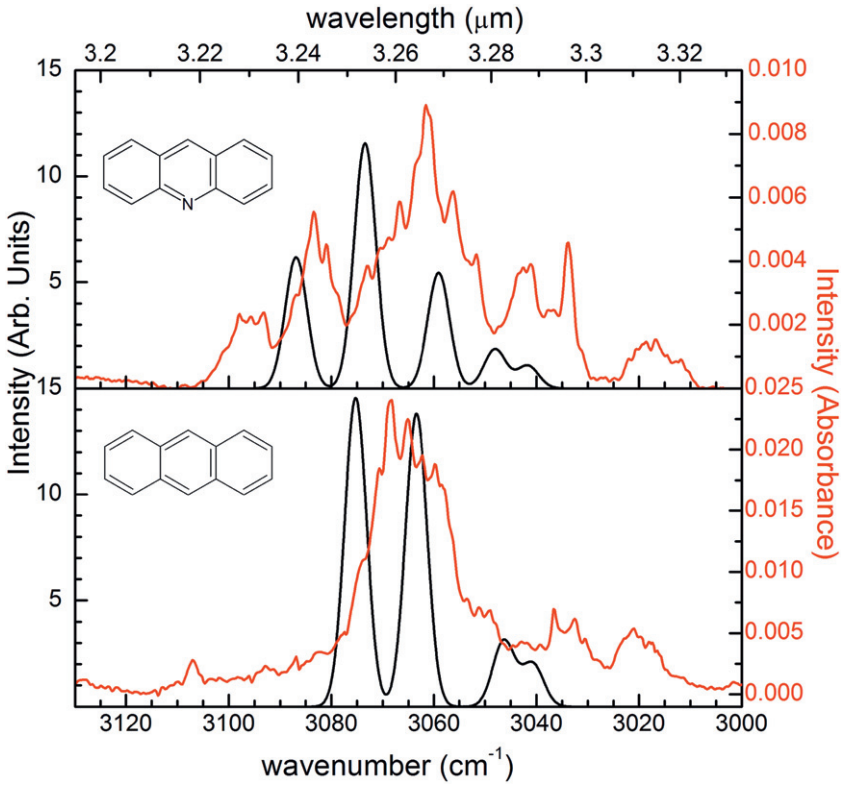

Fig. 10. The experimental (shown in red) and theoretical (B3LYP/6–31G(d) and shown in black) C–H stretching region for anthracene and acridine. Experimental spectra have been normalized to 1×10^{16} molecules.

we note that for 2-azabenz[a]anthracene, which does not have a hydrogen para to the nitrogen, there is a moderately strong band at 1451 cm^{-1} arising from the C–N–C asymmetric stretch. Therefore it appears that the nitrogen atom "lights up" at least one in-plane vibrational mode, but that the position of the enhanced emission can vary, usually between 1370 and 1400 cm^{-1} or between 1480 and 1515 cm^{-1} if there is a hydrogen para to the nitrogen, but as demonstrated by 2-azabenz[a]anthracene, for the species without a hydrogen para to the nitrogen it might fall between these two ranges. More examples are required to confirm this last observation.

3.3. CH Stretching Region (3000 to 3150 cm^{-1})

Figs. 10–13 display the C–H stretching region for the experimental and computational spectra. While the experimental bands are relatively broad, it is clear that they are composed of several overlapping bands and that these bands vary in number and position with the molecule. This is consistent with the notion that C–H stretching of the solo, duo, trio, and quartet hydrogens tend to fall at slightly different positions [42]. As has been shown previously, coupling of adjacent groups can shift their positions and change their intensities. In addition, it is known that the steric interactions between neighboring H atoms in bay regions blue shift the band positions. In this work we find that the presence of nitrogen atoms introduces more complexity into the bands in this region, with the effect of the nitrogen depending on the relative positions of the nitrogen and the neighboring CH groups. Because the experimental bands are broad, we use the computed bands and their associated vibrational vectors to demonstrate the effect of nitrogen on the C–H stretching spectra.

The computed and experimental spectra are shown in Figs. 10–13. Selected C–H stretching vibrational modes are shown in Fig. 14. The simplest molecule is anthracene and it has four infrared allowed C–H stretching modes that are shown in Fig. 14. The lowest frequency mode is mostly C–H solo stretching in character, while the others are mostly C–H quartet stretches. These four allowed modes overlap into a single broad band in the experimental spectrum, although a slight shoulder can be seen around 3050 cm^{-1}. The positions of these bands is quite typical of PAH molecules.

A comparison of anthracene and acridine shows some small changes in position and intensity of the four bands observed in anthracene and a new band at 3087 cm^{-1}. This new band arises from the stretches of the CH groups (4 and 6, molecule 1, Fig. 1) next to the nitrogen atom, where the symmetric stretch is shown in the Fig. 14; the asymmetric stretch is 0.5 cm^{-1} lower in energy. The origin of this shift to higher frequency is not obvious. At the same level of theory we find the frequency of CH^+ is 75 cm^{-1} higher than for CH, and for 9-fluroanthracene (note this uses the IUPAC numbering scheme for anthracene, this would be position 5 in Fig. 1) there is C–H stretching band at 3093 cm^{-1}. Therefore, we attribute the shift to higher frequency in acridine to charge withdrawal by the nitrogen atom. However, the change in the Mulliken charge on the carbons at positions 4 and 6 is about 0.05 e^-, so we cannot rule out other factors contributing to the shift.

The remaining pairs of equivalent C–H stretches (3 + 7, 2 + 8, and 1 + 9, see Fig. 1, molecule 1) also show the effect of the nitrogen substitution. These three pairs could be described as being trios or three pairs of solo stretches with some coupling; namely the six bands that arise from these hydrogens all show motion of all of the hydrogens, but for each band one pair of hydrogens show greater motion than the other two pairs of hydrogens. These motions give rise to the bands at 3074, 3059, and 3048 cm^{-1}. The solo band is at 3042 cm^{-1}, thus the nitrogen has had very little effect on the stretching frequency of the solo C–H group para to the nitrogen compared to the C–H stretch in anthracene. It appears that the two highest frequency bands in the experimental spectra are shifted by about 10 cm^{-1} to the blue compared with the computed bands. In addition,

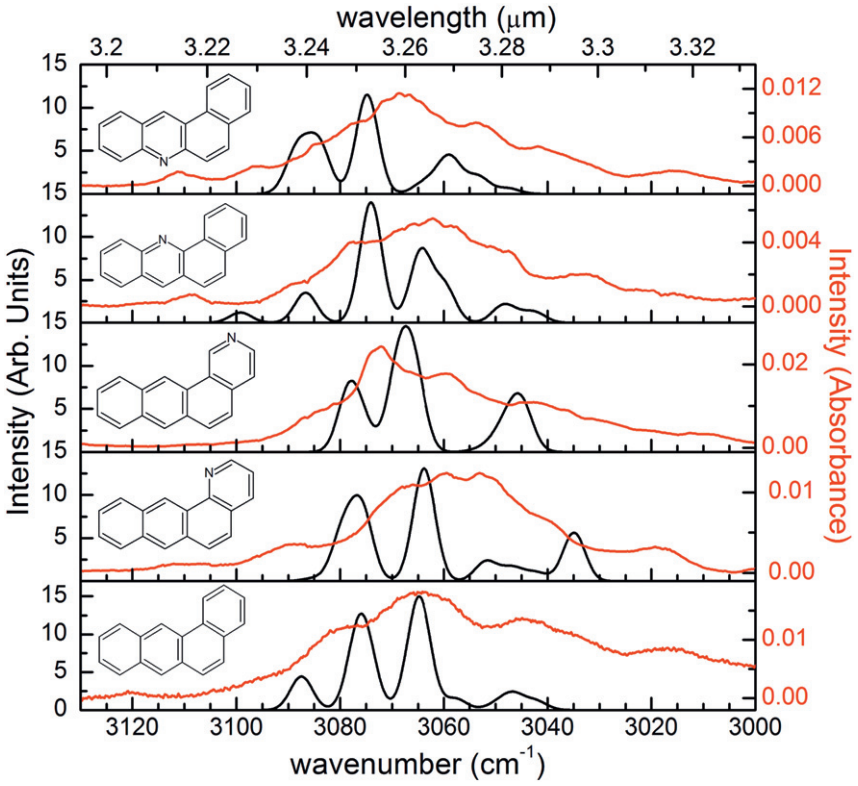

Fig. 11. The experimental (shown in red) and theoretical (B3LYP/6–31G(d) and shown in black) C–H stretching region for the species derived from benz[a]anthracene. Experimental spectra have been normalized to 1×10^{16} molecules.

the intensities of the 3074 and 3059 cm^{-1} bands seem to be reversed between the experimental and computed spectra. The experimental spectrum of anthracene, and most of the molecules in this study, contain a weak but clearly visible band around 3020 cm^{-1}. A recent study by Mackie et al. [43] identifies this as a combination band in benz[a]anthracene resulting from C–C stretches and C–H in-plane bends.

The benz[a]anthracene spectra (see Fig. 11) looks like anthracene with an extra band at 3087.5 cm^{-1}. The high frequency band is shown in Fig. 14 and is due to the symmetric stretch of the bay hydrogens (1 and 12, molecule 3, Fig. 1). Their stretch is shifted to higher energy due to the repulsive interaction of the hydrogens. Thus while both acridine and benz[a]anthracene have a high frequency band when compared to anthracene, they are quite different in character. The band 3075 cm^{-1} is composed of the C–H quartet stretches, while the band at 3065 cm^{-1} is mostly symmetric C–H duo stretches in character. The lowest frequency peak arises from bands with mixed character, but would be best described as being mostly asymmetric C–H duo stretching (the higher frequency component) and C–H solo (the lower frequency component). That is, the solo, that is not part of a bay, again falls at the lowest frequency. The experimental and computed spectra are in very good agreement.

The spectrum of 1-azabenz[a]anthracene does not appear to have the high frequency peak, but there is actually a very weak C–H(12) solo adjacent to the N at 3085 cm^{-1}. This is seen more clearly as a shoulder in the experimental spectrum in Fig. 11. The broad peak at about 3076 cm^{-1} is composed of a duo-like stretch of the C–H groups meta and para (3 and 4) to the nitrogen and the quartet C–H stretches. The band near 3064 cm^{-1} is derived from the quartet C–H and symmetric duo stretches. The broad band between 3052 and 3042 m^{-1} is mixed in character involving quartet, asymmetric duo, and finally solo C–H(7) stretches. The new band at 3035 cm^{-1} arises from the C–H(2) group ortho to the nitrogen. The experimental and computed spectra are in good agreement.

The spectra of 2-azabenz[a]anthracene does not show the C–H bay stretch as found for benz[a]anthracene. The peak at 3078 cm^{-1} is composed of the quartet C–H stretch and the solo hydrogen (12) ortho to the nitrogen, with essentially no contribution from the solo bay hydrogen. The band at 3066 cm^{-1} is composed of the two pairs of duo C–H stretches and C–H quartet stretches. The band at 3045 cm^{-1} is composed of the C–H(1) ortho to the nitrogen and C–H(7) solo stretches. Thus, we see a very strong nitrogen ortho effect on the C–H stretching frequencies. This ortho effect has been previously [44] observed for pyridine, where the C–H bond ortho to the N is 7 kcal/mol lower in energy than the C–H bonds meta and para to the N. The theoretical bands at 3078 and 3066 cm^{-1} are shifted slightly to the blue of their experimental positions, with the intensities of the bands being reversed.

The benz[c]acridine has two higher frequency peaks compared with anthracene. These two peaks involve the stretching of the CH groups adjacent to the nitrogen (1 and 11, Fig. 1, molecule 3) The highest frequency peak is shown in Fig. 14 and is like a bay stretch, but where the hydrogen (1) has a repulsive interaction with the nitrogen lone pair instead of another hydrogen. The other C–H(11) stretch is similar to that observed for acridine and, not surprisingly, falls at essentially the same frequency as found for acridine. The band at 3074 cm^{-1} is quartet C–H stretching in character, while the band near 3064 cm^{-1} is composed of several bands arising from duo and quartet C–H stretches. The lowest frequency peak is again mixed in character, being composed of quartet, asymmetric duo, and solo C–H stretches. The experimental and theoretical spectra are in good agreement with the high frequency band shifted about 10 cm^{-1} to the blue in the experimental spectrum and the intensity of the 3074 and 3066 cm^{-1} bands reversed.

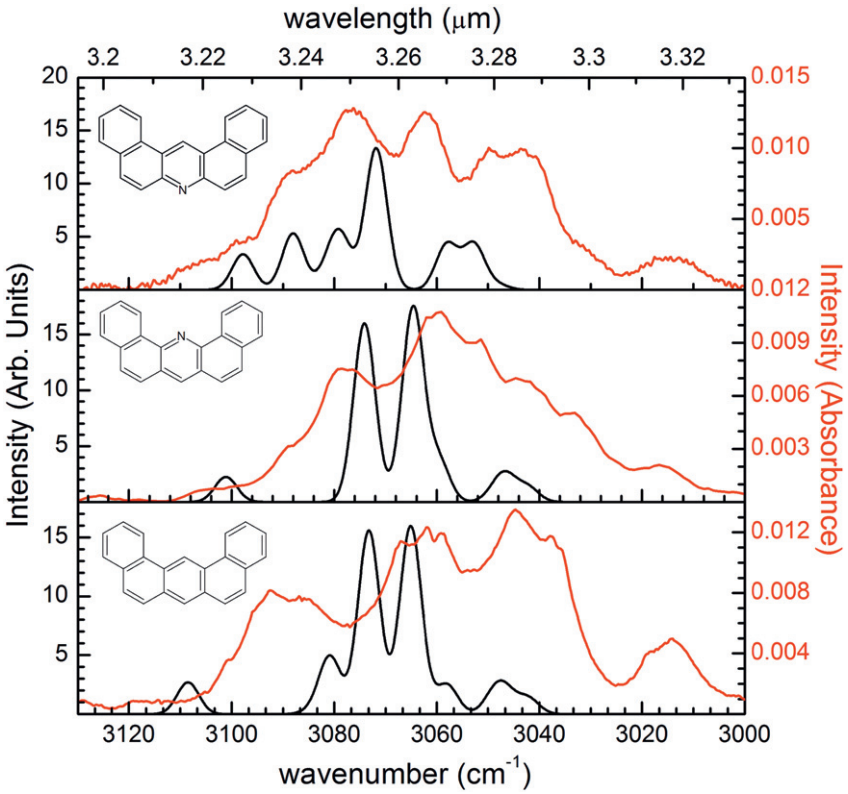

Fig. 12. The experimental (shown in red) and theoretical (B3LYP/6–31G(d) and shown in black) C–H stretching region for species derived from dibenz[a,j]anthracene. Experimental spectra have been normalized to 1×10^{16} molecules.

The computed spectra of benz[a]acridine has a very large high frequency peak that is composed of three vibrational modes, the symmetric and asymmetric stretches of the C–H groups next to the nitrogen (6 and 8, Fig. 1, molecule 3) and the symmetric bay hydrogen (1 and 12) stretch. That is, this sizable peak is essentially the superposition of the acridine and portions of the benz[a]anthracene spectra. As found for the other species in this series, the band at 3074 cm^{-1} is composed of the quartet C–H stretch. The broad feature running from 3064 to 3047 cm^{-1} is composed of several bands that involve asymmetric bay, the duo C–H(5) that is not adjacent to the nitrogen, and quartet stretches. Note for this molecule, the lowest frequency band is mostly quartet in character, unlike the others species where it is the solo stretch. This arises for benz[a]acridine since the only solo H has a bay interaction. The broad band, composed of three bands, at about 3055 cm^{-1} in the computed spectrum appears to be broken apart in the experimental spectrum.

The spectra of the dibenz species in Figs. 12 and 13 shows many of the same features shown in the anthracene and benz[a]anthracene derived species. The computed dibenz[a,j]anthracene spectra shows a band at 3108 cm^{-1} that is the symmetric combination of the two bay stretches, which is shown in Fig. 14. The internal C–C bond lengths are slightly longer than edge C–C bond lengths, which pushes the bay hydrogens closer together and shift their symmetric stretch to slightly higher frequency than found for the benz[a]anthracene. The band at 3081 cm^{-1} band is composed of the other two components of the bay stretches, which are also shown in Fig. 14. These are the very weak asymmetric C–H 1 and 13 stretches at 3084.3 cm^{-1} and strong combination of the symmetric stretch of C–H groups 1 and 13 with the out-of-phase stretch of the central C–H(14) stretch at 3080.9 cm^{-1}(Fig. 1, molecule 8). The strong band at 3073 cm^{-1} is a quartet stretch, while the strong band at 3065 cm^{-1} arises from the symmetric duo stretches. The bands at lower frequency are quartet, asymmetric duo, and finally solo in character. The experimental spectrum, at first glance, appears to be somewhat different from the computed spectrum. However, as discussed previously, the 3074 cm^{-1} mode, mostly quartet in character, tends to be shifted by about 10 cm^{-1} to the blue in the experimental spectrum and the intensities of the 3074 and 3065 cm^{-1} bands tend to be reversed. The mixed mode bands between 3050 and 3040 cm^{-1} are more intense than predicted by theory.

Changing the central C–H into an nitrogen to form dibenz[c,h]acridine reduces the number of bay stretches from three to two and these coalesce into a single band, because the nitrogen lone pair is stationary. The remaining bands are very similar in position and character as in the parent. There is excellent agreement between the experimental and theoretical spectra.

Switching the location of the nitrogen from the top of the ring to the bottom to form dibenz[a,j]acridine causes some significant changes to the spectra. The totally symmetric bay stretch shifts down in frequency to 3098 cm^{-1} because the C–N bonds are slightly shorter than the C–C bonds which tilts the top two rings away from each other and hence slightly reduces the bay H repulsive interaction. The band at 3088 cm^{-1} is composed of the symmetric and asymmetric stretches of the CH(6 and 8) groups next to the nitrogen (see Fig. 1, molecule 8), i.e. the same bands as found at 3087 cm^{-1} in acridine. The band at 3079 cm^{-1} is composed of the other two combinations of the bay hydrogens, which also falls at slightly lower frequency than in dibenz[a,j]anthracene. Since the nitrogen splits the duo stretch into effectively two solo stretches, the symmetric duo stretch band is missing and only the lower frequency bands appear in the spectra that are essentially solo H 5 and 9 stretches. Note that since the only solo hydrogen is involved in a bay interaction, the band does not extend to as low a frequency as found in dibenz[a,j]anthracene and dibenz[c,h]acridine. The experimental

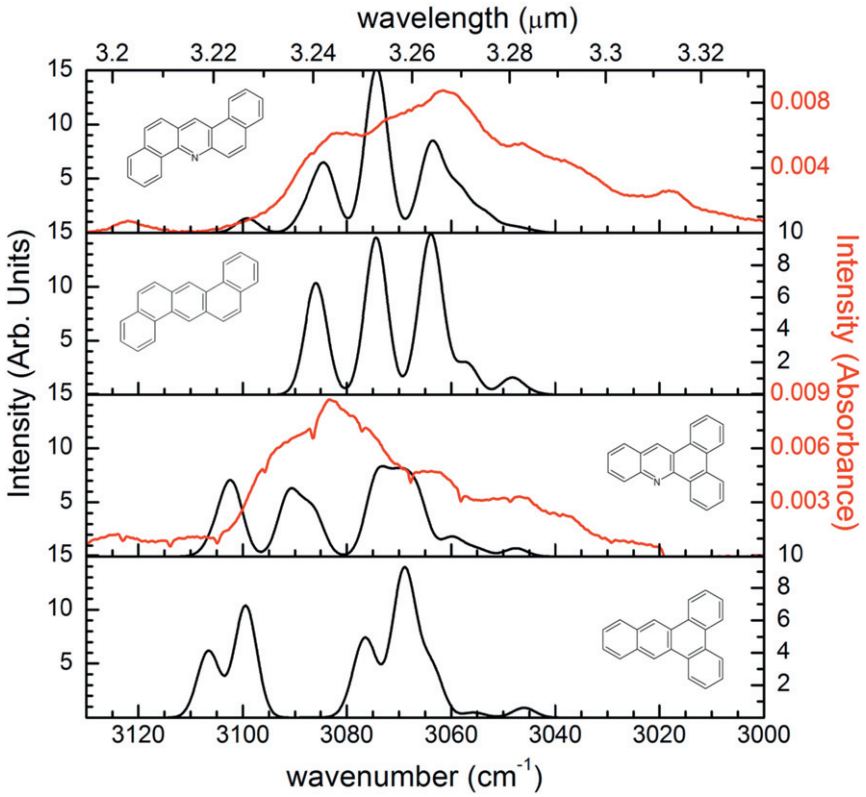

Fig. 13. The experimental (shown in red) and theoretical (B3LYP/6–31G(d) and shown in black) C–H stretching region for species derived from dibenz[a,h]anthracene and dibenz[a,c]anthracene. Experimental spectra have been normalized to 1×10^{16} molecules.

and computed spectra are in good agreement with less than 10 cm^{-1} shifts in the lower frequency mixed mode.

In dibenz[a,h]anthracene (see Fig. 13), the two C–H bay bands do not interact and therefore fall at 3086 cm^{-1}, which is lower than in dibenz[a,j]anthracene, but very similar to benz[a]anthracene. The remaining bands have the expected character, namely quartet stretch at 3074 cm^{-1}, symmetric duo stretch at 3064 cm^{-1}, followed by the weaker bands composed of quartet and asymmetric duo stretches. Substituting a nitrogen adds a band at 3099 cm^{-1}, which is N–C–H(8) bay-like stretch. The band at 3085 cm^{-1} is composed of the normal C–H(1 and 14) symmetric bay stretch and the C–H(6) stretch for the group adjacent to the N, as found in acridine (see Fig. 1, molecule 11). The band at 3074 cm^{-1} is the typical quartet stretch and the 3064 cm^{-1} is symmetric duo and asymmetry bay stretches. The asymmetric duo and quartet stretches form the red wing of this band. Since the only solo is part of bay interaction, there is no low frequency solo component.

Dibenz[a,c]anthracene has bands at 3107, 3100, and 3099 cm^{-1} that arise from the three bays stretches. The highest frequency band corresponds to the stretch of H 4 and 5 (Fig. 1, molecule 13). Because internal C–C bond length (i.e. a bond between two carbons that are bonded to two other carbons and no hydrogens) is slightly longer than an edge length, these bands fall near those of dibenz[a,j]anthracene and higher than that in benz[a]anthracene. The bands at 3077 and 3069 cm^{-1} are composed of quartet and asymmetric bay stretches. The red shoulder on the 3069 cm^{-1} is mostly quartet stretching in character and the remaining bands are very weak.

The spectra of dibenz[a,c]acridine shows some significant changes relative to its parent. The bands at 3105, 3102, 3091, and 3087 cm^{-1} correspond to bay hydrogen 8-N interaction, bay hydrogens 4 and 5, bay hydrogens 1 and 14, and the hydrogen (10) next to the N (i.e. stretch noted for acridine), respectively. The broad band that stretches from 3074 to 3060 cm^{-1} is composed of quartet and asymmetric bay stretches. The lower frequency bands are weak as found for the parent. The theoretical and experimental spectra are in good agreement.

In this subsection, we have shown that the substitution of nitrogen for a CH group makes more significant changes in the C–H stretching region than might have been expected. The nitrogen can shift an adjacent C–H stretch to higher frequency as found for acridine and several other species. However, we also found that nitrogen can shift a hydrogen at the ortho position to lower frequency. For example in 1-azabenz[a]anthracene where the nitrogen splits the expected trio stretch into a solo-like and duo-like stretches, where the solo at the ortho position falls at lower frequency that a typical trio. A second example is 2-azabenz[a]anthracene where the nitrogen shifts the bay hydrogen ortho to the nitrogen to a frequency lower than a typical bay stretch to a frequency only slightly higher than in a typical quartet stretch. The nitrogen lone pair can interact with a C–H stretch to create a bay-like stretch. Clearly nitrogen can affect the C–H stretching region in many ways. A summary of the positions for the various types of C–H stretches is shown in Fig. 15.

4. Conclusions

This work builds on the earlier investigations concerning PANHs, namely nitrogen containing PAHs. As noted in previous work, the presences of a nitrogen atom within the PAH skeleton disrupts the electron distribution within the entire PANH molecule, resulting in a two-fold increase in the band intensity visible in the 1000–1600 cm^{-1} region. Likewise we note the presence of an intense band

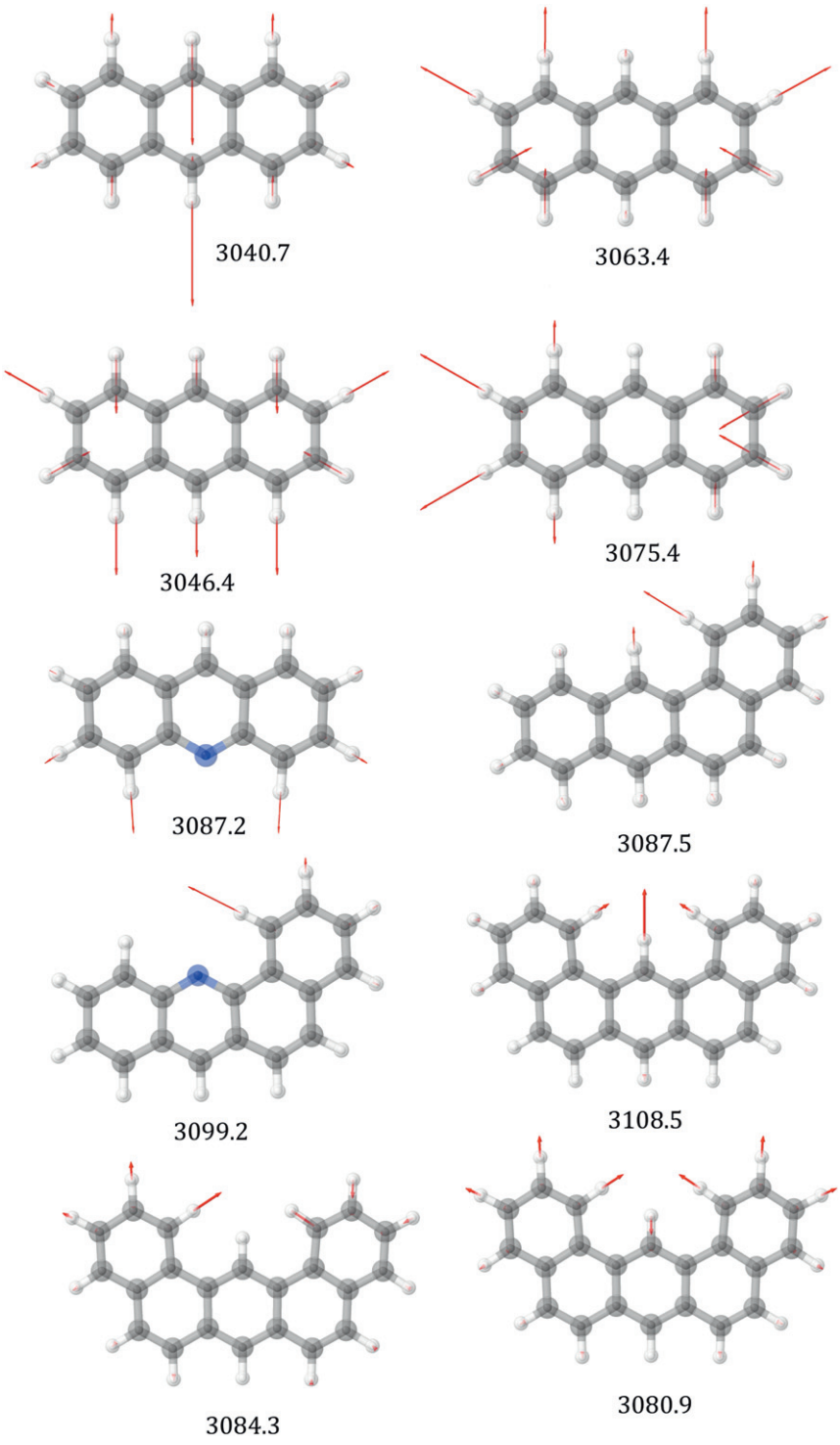

Fig. 14. Selected B3LYP/6–31G(d) vibrational modes.

around 1400 cm^{-1}, due to the in-plane wagging motion of a hydrogen atom opposite that of a C–N–C rocking motions, similar to what we observed in earlier studies. A feature, similar in intensity to the C–N–C with in-plane hydrogen wagging, is noted around 1480 to 1515 cm^{-1} and is the result of an in-plane hydrogen wag in conjunction with a C–N–C stretching motion. These C–N–C rocking and stretching motions may serve as unique fingerprints for the PANH molecules. The in-plane modes of the 1375–1600 cm^{-1} region are primarly responsible for the observed increase in intensity observed for the entire in-plane region (i.e. 1100–1600 cm^{-1}). Thus, PANH molecules may contribute to the variability observed in the astronomical 6.2 to 7.2 μm features.

The addition of benzene rings to the anthracene or acridine substructure results in several interesting observations for the CH_{oop} region. First, for the benz[a]anthracene series, the addition of a benzene ring almost doubles the number of skeletal modes visible in

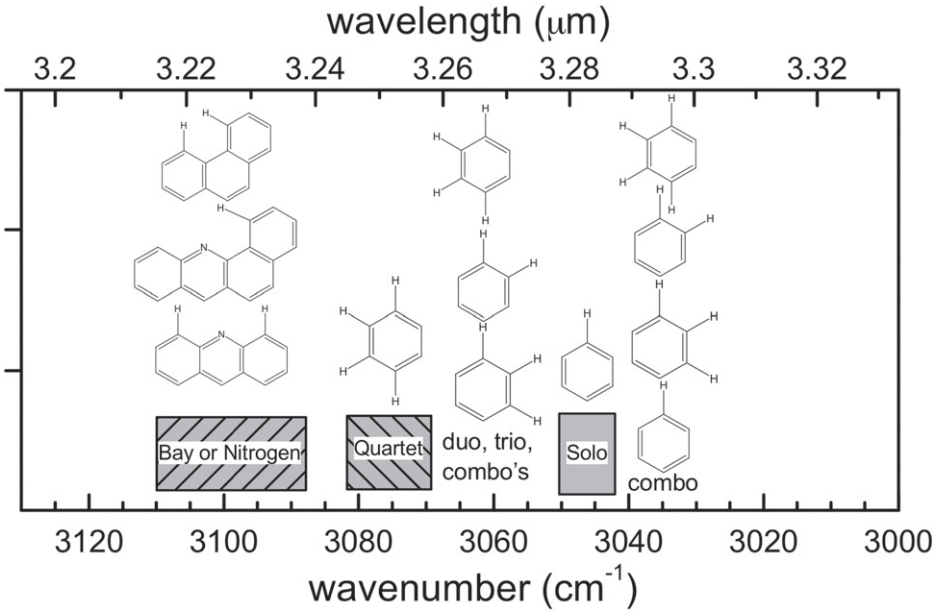

Fig. 15. Summary of the positions for the various type of C–H stretches.

the infrared spectrum between 450 and 700 cm^{-1}. The insertion of nitrogen into this series leads to the shifting of some of the bands in this region but not to a drastic change in number. While the addition of a second benzene ring, forming the dibenz[a,j]anthracene series, increases the number of skeletal modes in this region, it is not to the extent observed in the benz[a]anthracene series.

The insertion of nitrogen and the addition of benzene rings to the anthracene structure result in a somewhat combined effect for the solo, duo, and quartet regions. Insertion of nitrogen into the acridine position (i.e. in the anthracene ring) shifts the quartet hydrogen modes to the blue for the acridine series of molecules while insertion into an adjacent benzene ring, 1- and 2-azabenz[a]anthracene, shifts the quartet hydrogen mode to the red of the parent PAH. Addition of the first benzene ring shifts the quartet hydrogen mode to the blue from anthracene, while the addition of a second benzene ring shifts the quartet mode to the red, but not all the way back to the position observed in anthracene's spectrum. The duo and solo hydrogen modes seem to be more sensitive to the insertion and position of nitrogen, with the addition of benzene rings building on this impact. Addition of the first benzene ring creates a bay region in the PAH, resulting in a bay region solo hydrogen and an external solo hydrogen. The bay region hydrogen seems to interact and couple with the quartet hydrogen motions while the external hydrogen couples with the duo hydrogen atoms adjacent to it in the PAH/PANH skeleton. This results in progressive shifting to the blue of the solo hydrogen motion with each addition of a benzene ring, while the position of the duo hydrogen motion seems invariant to the addition benzene ring. This interaction is exemplified by the replacement of the bay solo hydrogen with a nitrogen atom. The duo hydrogen motions seem unaffected by this change; whereas replacement of the external solo hydrogen atom shifts the duo hydrogen motions to the blue. In all instances of this investigation, replacement of a solo hydrogen from the anthracene base, creating an acridine, shifts the solo hydrogen motion to the blue. However, in the instances of dibenz[a,j]acridine, dibenz[a,c]acridine, and benz[a]acridine the solo hydrogen mode is extremely weak. We believe this is due to the external solo hydrogen being replaced by a nitrogen atom. Upon formation of a bay region, separating the bay region solo hydrogen and the external solo hydrogen motion, the external hydrogen seems to be primarily responsible for the solo hydrogen mode visible in the infrared spectrum. Thus when this group is replaced by a nitrogen atom, the solo hydrogen motion intensity drastically decreases.

The C–H stretching region appears to behave similar to what we observed in our dibenzopolyacene investigation, with the solo hydrogen motion, coupled to the duo hydrogens, being responsible for the weak, low frequency features between 3000 and 3020 cm^{-1}, the quartet hydrogens providing the most intense C–H stretches around 3065 cm^{-1} and the duo hydrogens coupling with the quartet hydrogens and contributing to the features between 3025 and 3050 cm^{-1}. The splitting of the bay region solo hydrogen from the external solo hydrogen is also evident in the theoretical calculations, with the external solo hydrogen combining with the duo hydrogens to form the lowest frequency mode and the highest frequency modes due to the coupling between the quartet hydrogens and the bay region solo hydrogen. The consistent position of the quartet hydrogens C–H stretching mode could potentially serve as a compact versus open PAH structure diagnostic tool in higher resolution spectroscopic data (astronomical or terrestrial). Likewise, the presence of the higher frequency modes (>3095 cm^{-1}) could serve as an indicator of nitrogen's presence in the PAH structure or the presence of a bay region in the PAH.

In summary, this work reveals that the creation of bay regions in a PAH molecule splits the solo hydrogen motions, with the bay solo hydrogen coupling with quartet hydrogens while the external solo hydrogen couples with the adjacent duo hydrogen motions. Nitrogen's presence and position in the PAH skeleton impacts PAH band positions and intensities, which could serve to help form an identification protocol to distinguish between PAHs and PANHs.

Acknowledgments

The authors wish to acknowledge the expert technical support of Bob Walker. This work was fully supported by NASA's Exobiology and Astrobiology programs, under grants 11-EXO-0073,13-13NAI7_2-0039 and NNX13AJ08G.

References

[1] C.A. Menzie, B.B. Potocki, J. Santodonato, E.S.&T. 26 (1992) 1279.
[2] P. Cox, M. Kessler, The Universe as Seen by ISO ESA SP 427, ESTEC Noordwijk, The Netherlands, 1999.
[3] E.F. van Dishoeck, Organic matter in space -An overview, IAU Symp. No. 251, 2008, pp. 3.
[4] C. Oblin, A.G.G.M. Tielens, PAHs and the Universe, EDP Sciences, France, 2011.
[5] A. Omont, A&A 164 159–478.
[6] L. Zhang, P. Li, Z. Gong, X. Li, J. Hazard. Mater. 158 (2008) 478–484.
[7] X. Huang, Y. El-Alwai, D.M. Penrose, B.R. Glick, B.M. Greenberg, Environ. Pollut. 130 (2004) 465–476.
[8] A.G. Chmielewski, Y. Sun, S. Bulka, K. Kubica, Z. Zimek, Radiat. Phys. Chem. 67 (2003) 555–560.
[9] A.G. Chmielewski, A. Ostapczuk, Z. Zimek, J. Licki, K. Kubica, Radiat. Phys. Chem. 63 (2002) 653–655.
[10] C.K. Materese, D.P. Cruikshank, S.A. Sandford, H. Imanaka, M. Nuevo, D. White, ApJ 788 (2014) 111.
[11] D.P. Cruikshank, C.M. Dalle Ore, R.N. Clark, Y.J. Pendleton, Icarus 233 (2014) 306–315.
[12] B. Markert, S. Franzle, S. Wunschmann, Chemical Evolution, Present and Future Projects on Chemical Evolution by Means of Space Research, Springer. 2014, 197–207.
[13] F. Capaccioni, et al. Science 347 (2015) 628–1.
[14] M.P. Bernstein, A.L. Mattioda, S.A. Sandford, D.M. Hudgins, ApJ 626 (2005) 909.
[15] S.B. Charnley, Y.-J. Kuan, H.-C. Huang, et al. AdSpR 36 (2005) 137.
[16] C.W. Bauschlicher, E. Peeters, L.J. Allamandola, ApJ 697 (2009) 311.
[17] M. Saito, Y. Kimura, Y. ApJL 703 (2009) L147.
[18] J.Y. Bonnet, E. Quirico, A. Buch, et al. Icarus 250 (2015) 53.
[19] H. Imanaka, B.N. Khare, J.E. Elsila, et al. Icarus 168 (2004) 344.
[20] T.B. McCord, G.B. Hansen, B.J. Buratti, et al. P&SS, 54. 2006, 1524.
[21] E. Quirico, G. Montagnac, V. Lees, et al. Icarus 198 (2008) 218.
[22] Y.S. Kim, R.I. Kaiser, ApJS 181 (2009) 543.
[23] A. Landera, A.M. Mebel, FaDi, 147. 2010, 479.
[24] C.M. Dalle Ore, M. Fulchignoni, D.P. Cruikshank, et al. A&A, 533. 2011, A98.
[25] D.P. Cruikshank, W.M. Grundy, F.E. DeMeo, et al. Icarus 246 (2015) 82.
[26] A.L. Mattioda, D.M. Hudgins, C.W. Bauschlicher, L.J. Allamandola, Adv. Space. Res. 36 (2005) 156–165.
[27] A.L. Mattioda, D.M. Hudgins, C.W. Bauschlicher, M. Rosi, L.J. Allamandola, J. Phys. Chem. A 107 (2003) 1486.
[28] D.M. Hudgins, S. Sandford, J. Phys. Chem. A 102 (1998) 329.
[29] J.G. Redziszewski, J. Michel, J. Phys. Chem. 82 (1985) 3527.
[30] M.B. Mitchell, G.R. Smith, W.A. Guilloy, J. Chem. Phys. 75 (1981) 44.
[31] A.D. Becke, J. Chem. Phys. 98 (1993) 5648.
[32] P.J. Stephens, F.J. Devlin, C.F. Chabalowski, M.J. Frisch, J. Phys. Chem. 98 (1994) 11623.
[33] M.J. Frisch, J.A. Pople, J.S. Binkley, J. Chem. Phys. 80 (1984) 3265. (and references therein).
[34] C.W. Bauschlicher, S.R. Langhoff, Spectrochim. Acta A 53 (1997) 1225.
[35] C.W. Bauschlicher, A. Ricca, A., Mol. Phys. 108 (2010) 2647.
[36] T.H. Dunning, J. Chem. Phys. 90 (1989) 1007–1023.
[37] O. Pirali, M. Vervloet, G. Mulas, G. Malloci, C. Joblin, Phys. Chem. Chem. Phys. 11 (2009) 3443.
[38] D.M. Hudgins, S.A. Sanford, J. Phys. Chem. A 102 (1998) 329.
[39] J. Szczepanski, M. Vala, ApJ 414 (1993) 646.
[40] M.J. Frisch, et al. Guassian 09 Revision D. 01, Gaussian, Inc., Wallingford CT, 2010.
[41] Jmol: an open-source Java viewer for chemical structures in 3D., http://www.jmol.org/.
[42] A.L. Mattioda, C.W. Bauschlicher, J.D. Bregman, D.M. Hudgins, L.J. Allamandola, A. Ricca, Spectrochim. Acta A Mol. Biomol. Spectrosc. 130 (2014) 639.
[43] C.J. Mackie, A. Candian, X. Huang, E. Maltseva, A. Petrignani, J. Oomans, A.L. Mattioda, W.J. Bama, T.J. Lee, A.G.G.M. Tielens, J. Chem. Phys. submitted.
[44] J.H. Kiefer, Q. Zhang, R.D. Kern, J. Yao, B. Jursic, J. Phys. Chem. A 101 (1997) 7061.